ERDC/CRREL MP-21-22

US Army Corps
of Engineers®
Engineer Research and
Development Center

Extra-Wide-Angle Parabolic Equations in Motionless and Moving Media

Vladimir E. Ostashev, Michael B. Muhlestein,
and D. Keith Wilson

September 2021

Cold Regions Research and Engineering Laboratory

The U.S. Army Engineer Research and Development Center (ERDC) solves the nation's toughest engineering and environmental challenges. ERDC develops innovative solutions in civil and military engineering, geospatial sciences, water resources, and environmental sciences for the Army, the Department of Defense, civilian agencies, and our nation's public good. Find out more at www.erdc.usace.army.mil.

To search for other technical reports published by ERDC, visit the ERDC online library at https://erdclibrary.on.worldcat.org/discovery.

ERDC/CRREL MP-21-22
September 2021

Extra-Wide-Angle Parabolic Equations in Motionless and Moving Media

Vladimir E. Ostashev, Michael B. Muhlestein, and D. Keith Wilson

Cold Regions Research and Engineering Laboratory
U.S. Army Engineer Research and Development Center
72 Lyme Road
Hanover, NH 03755

Final report

Prepared for U.S. Army Corps of Engineers
Washington, DC 201314

Under Geospatial Research and Engineering and Military Engineering

Preface

This research was sponsored by the U.S. Army Engineer Research and Development Center, Geospatial Research and Engineering and Military Engineering business areas.

The work was performed by the U.S. Army Engineer Research and Development Center, Cold Regions Research Engineering Laboratory (ERDC-CRREL). At the time of publication of this paper, the Deputy Director for ERDC-CRREL was Mr. David Ringelberg and the Director was Dr. Joseph Corriveau.

This article was originally published online in the *Journal of the Acoustical Society of America* on 25 February 2019.

The Commander of ERDC was COL Teresa A. Schlosser and the Director was Dr. David W. Pittman.

Extra-wide-angle parabolic equations in motionless and moving media

ABSTRACT

Wide-angle parabolic equations (WAPEs) play an important role in physics. They are derived by an expansion of a square-root pseudo-differential operator in one-way wave equations, and then solved by finite-difference techniques. In the present paper, a different approach is suggested. The starting point is an extra-wide-angle parabolic equation (EWAPE) valid for small variations of the refractive index of a medium. This equation is written in an integral form, solved by a perturbation technique, and transformed to the spectral domain. The resulting split-step spectral algorithm for the EWAPE accounts for the propagation angles up to 90° with respect to the nominal direction. This EWAPE is also generalized to large variations in the refractive index. It is shown that WAPEs known in the literature are particular cases of the two EWAPEs. This provides an alternative deri-vation of the WAPEs, enables a better understanding of the underlying physics and ranges of their applicability, and opens an opportunity for innovative algorithms. Sound propagation in both motionless and moving media is considered. The split-step spectral algorithm is particularly useful in the latter case since complicated partial derivatives of the sound pressure and medium velocity reduce to wave vectors (essentially, propagation angles) in the spectral domain.

https://doi.org/10.1121/1.5091011

I. INTRODUCTION

Several areas of physics require accurate and robust algorithms for wave propagation at large angles with respect to the nominal direction. Wide-angle propagation occurs in three main cases: (i) sound waves are reflected from boundaries of a medium, (ii) the sound wavelength is comparable to the scale of medium inhomogeneities, thus resulting in scattering at large angles, and (iii) the refractive index of a medium changes significantly in the direction perpendicular to the nominal. Wide-angle parabolic equations (WAPEs) have been widely used to address these cases in geophysics,[1] ocean acoustics,[2–6] atmospheric acoustics,[7–11] non-linear acoustics,[12,13] and electromagnetic wave propagation.[14–16] WAPEs are usually obtained by an expansion of a square-root pseudo-differential operator in a one-way wave equation; the resulting equations are then solved with finite-difference techniques.[1,2,5] Note that the terms "one-way wave equation" and "WAPE" are used in this paper mostly as synonyms; in some cases, the former indicates a starting equation and the latter, the final result of manipulations.

This paper suggests a new approach for WAPEs. The starting point is a one-way wave equation derived by Ostashev and Tatarskii,[17,18] which is applicable for small variations of the refractive index. If these variations tend to zero, the equation correctly accounts for propagation angles up to 90° with respect to the nominal direction. Since the maximum propagation angle for a WAPE is typically around 40°, this equation is called here an extra-wide-angle parabolic equation (EWAPE). It enables us to consider cases (i) and (ii) formulated above. In this paper, the EWAPE is written in an integral form, solved by a perturbation technique (for a small range step), and transformed into the spectral domain. This approach is termed as a split-step spectral algorithm for the EWAPE. In the limiting case of narrow propagation angles, this approach coincides with the well-known split-step Fourier algorithm.[5]

In the split-step spectral algorithm, two integrals need to be evaluated at each range step. If we assume that the sound wavelength is smaller than the scale of medium inhomogeneities, one of the integrals can be calculated analytically. The resulting split-step algorithm for the EWAPE enables us to consider case (i). Numerical implementation of the split-step algorithm is discussed.

The EWAPE is also generalized to account for large variations in the refractive index, which enables us to consider cases (i) and (iii). This new EWAPE can be solved by the split-step spectral algorithm. The two EWAPEs are then applied for sound propagation in the atmosphere above an impedance ground. The resulting equations are termed as extra-wide-angle Green's function parabolic equations (GFPEs).

Under certain approximations, the two EWAPEs reduce to WAPEs known in the literature. This is an important methodological result, which provides an alternative derivation of the WAPEs and enables better understanding of the underlying physics of these equations and their ranges of applicability. In particular, in the literature, WAPEs are usually obtained by omitting some terms in partial differential equations; the physical meaning and ranges of applicability

of the resulting approximations are often difficult to access. When the WAPEs are derived from the EWAPEs as in the current paper, the approximations involved have a clear physical meaning and their ranges of applicability can be readily studied.

Another advantage of the EWAPEs is that they significantly simplify formulations for sound propagation in a moving medium by replacing many partial derivatives of the sound pressure and medium velocity appearing in WAPEs (e.g., Refs. 7, 8, and 11) with wave vectors (essentially, propagation angles) in the spectral domain. The EWAPEs also open an opportunity for developing new approaches. Based on this formalism, new WAPEs in motionless and moving media are suggested.

Most formulations in this paper are done in a three-dimensional (3D) Cartesian coordinate system. The case of 3D propagation is often considered in cylindrical coordinates,[19,20] for which cross-term operators become problematic.[5] In the split-step spectral algorithm, this problem does not occur.

The paper is organized as follows. In Sec. II, the geometry of the problem is formulated, and WAPEs known in the literature are briefly overviewed. Section III considers the EWAPEs for small and large variations of the refractive index in a motionless medium. In Sec. IV, the split-step spectral algorithm for solving the EWAPEs are developed. The ranges of applicability of the EWAPEs and WAPEs are studied in Sec. V. Sound propagation in the atmosphere above an impedance ground is considered in Sec. VI. EWAPEs in a moving medium with variable density are analyzed in Sec. VII. The results obtained are summarized in Sec. VIII.

II. STARTING EQUATIONS

In this section, the geometry of the problem is formulated, starting equations are presented, and WAPEs used in the literature are briefly overviewed.

A. Geometry of the problem

The geometry of the problem is shown in Fig. 1. A harmonic sound wave propagating in the direction of the x axis is incident on an inhomogeneous medium located in the space $x > x_0$. At the plane $x_0 = \text{const}$, the sound pressure of this wave, $p(x_0, \mathbf{r})$, is known. Here, $\mathbf{r} = (y, z)$ are the transverse coordinates. The sound pressure $p(x_0, \mathbf{r})$ can also correspond to a point source located in this plane. The goal is to calculate the sound pressure $p(x, \mathbf{r})$ inside the medium accounting for wide-angle propagation.

Inside the medium, the sound pressure satisfies the Helmholtz equation,

$$\left[\frac{\partial^2}{\partial x^2} + \frac{\partial^2}{\partial \mathbf{r}^2} + k_0^2[1 + \varepsilon(\mathbf{R})]\right] p(\mathbf{R}) = 0, \tag{1}$$

where $\mathbf{R} = (x, \mathbf{r}) = (x, y, z)$ are the Cartesian coordinates and $\varepsilon = N^2 - 1$ describes the deviation of the refractive index $N = c_0/c$ from unity. Here, c is the sound speed, c_0 is its reference value, $k_0 = \omega/c_0$ is the reference wavenumber, and ω is the sound frequency.

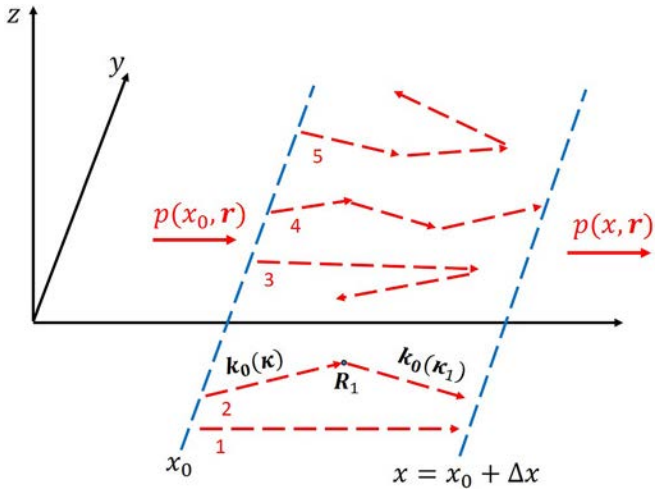

FIG. 1. (Color online) Geometry of sound propagation and scattering in the 3D slab between the planes $x_0 = \text{const}$ and $x = x_0 + \Delta x = \text{const}$. The sound fields at the left and right boundaries of the slab are $p(x_0, \mathbf{r})$ and $p(x, \mathbf{r})$. Diagram 1 corresponds to the sound wave propagating through the slab without scattering. Diagrams 2 and 4 indicate sound waves scattered forward, and diagrams 3 and 5 correspond to sound waves with backscattering. For diagram 2, scattering occurs at the point $\mathbf{R}_1 = (x_1, \mathbf{r}_1)$.

B. Conventional derivation of WAPEs

For the considered problem, WAPEs are usually derived by the following approach (e.g., Refs. 1, 2, and 5). Equation (1) is written in the form

$$\left\{\left(\frac{\partial}{\partial x} + ik_0\hat{Q}\right)\left(\frac{\partial}{\partial x} - ik_0\hat{Q}\right) + ik_0\left[\frac{\partial}{\partial x}, \hat{Q}\right]\right\} p(x, \mathbf{r}) = 0. \tag{2}$$

Here, the pseudo-differential operator $\hat{Q}$ is defined as

$$\hat{Q} = \sqrt{1 + \hat{\mu} + \varepsilon}, \tag{3}$$

where $\hat{\mu}$ is the differential operator,

$$\hat{\mu} = \frac{1}{k_0^2}\frac{\partial^2}{\partial \mathbf{r}^2}. \tag{4}$$

In Eq. (2), $[\partial/\partial x, \hat{Q}]$ is a commutator of the two operators, $\partial/\partial x$ and $\hat{Q}$. Omission of this commutator, yields a one-way wave equation

$$\left(\frac{\partial}{\partial x} - ik_0\hat{Q}\right) p(x, \mathbf{r}) = 0. \tag{5}$$

In the literature, the operator $\hat{Q}$ in Eq. (5) is approximated. Assuming that $\varepsilon + \hat{\mu}$ is small in comparison with unity, the operator $\hat{Q}$ can be approximated with the first two terms of a Taylor series

$$\hat{Q} = 1 + \hat{\mu}/2 + \varepsilon/2. \tag{6}$$

Substitution of $\hat{Q}$ into Eq. (5) results in a narrow-angle parabolic equation (PE)

$$\left[\frac{\partial}{\partial x} - ik_0(1 + \hat{\mu}/2 + \varepsilon/2)\right] p(x, \mathbf{r}) = 0. \tag{7}$$

The PE enables us to consider the angles θ between the direction of sound propagation and the x axis (see Fig. 2), which are less than or about 20°, e.g., Sec. 6.2.4 in Ref. 5.

A WAPE is usually obtained by also assuming that $\varepsilon + \hat{\mu}$ is small, but using a Padé (n,n) approximation for $\hat{Q}$ (e.g., Ref. 5),

$$\hat{Q} = 1 + \sum_{j=1}^{n} \frac{a_{j,n}(\varepsilon + \hat{\mu})}{1 + b_{j,n}(\varepsilon + \hat{\mu})}, \tag{8}$$

where $a_{j,n}$ and $b_{j,n}$ are coefficients. For the Padé (1,1) approximation ($n = 1$), Claerbout[1] suggests the following coefficients: $a_{1,1} = 1/2$ and $b_{1,1} = 1/4$. The corresponding WAPE enables us to consider the propagation angles θ up to 35°. The larger n is in Eq. (8), the wider the propagation angle that can be considered. This, of course, comes with increased complexity of the corresponding code and computational costs.

In optics, Feit and Fleck[16] suggested the following expansion of the operator $\hat{Q}$:

$$\hat{Q} = \sqrt{1 + \hat{\mu}} + \sqrt{1 + \varepsilon} - 1. \tag{9}$$

This approximation is used in ocean acoustics.[21] Other approximations of the operator $\hat{Q}$ are also considered in the literature, e.g., Ref. 22.

The PE, Eq. (7), is widely used for both analytical and numerical studies of wave propagation. WAPEs are usually used in numerical simulations. Generally, they are efficient if the propagation angle θ is not too large (less than about 45°).

III. EWAPE IN A MOTIONLESS MEDIUM

To account for large propagation angles, EWAPEs can be used. The first EWAPE (designated here as EWAPE1) is valid for small deviations of the refractive index from unity, when $|\varepsilon(x, \mathbf{r})| \ll 1$. This condition is not needed for the second EWAPE (designated EWAPE2), which is valid if $\varepsilon(x, \mathbf{r})$ is a slowly varying function of the transverse coordinates $\mathbf{r}$.

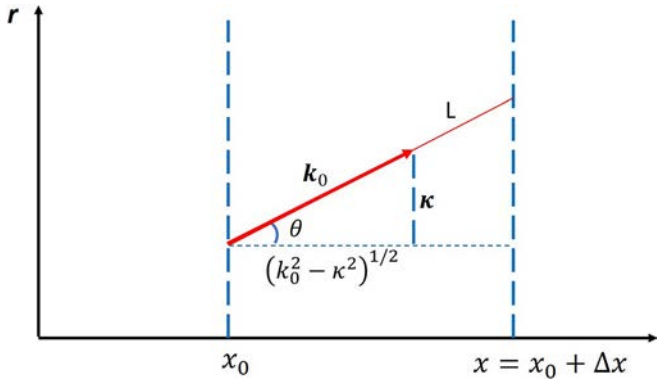

FIG. 2. (Color online) One of the plane waves in the spectral decomposition of $p(x, \mathbf{r})$. The vector $\mathbf{k}_0(\boldsymbol{\kappa})$ indicates the direction of its propagation within the 3D slab between the planes $x_0 = \text{const}$ and $x = x_0 + \Delta x = \text{const}$. Here θ is the propagation angle with respect to the x axis.

A. EWAPE1

For sound propagation in the atmospheric boundary layer and ocean, ε is usually small. In this subsection, we consider the application of EWAPE1 for this case.[17,18]

This equation was originally derived by an approach quite different from those for WAPEs. The Helmholtz equation (1) can be written in the following integral form:

$$p(x, \mathbf{r}) = p_0(x, \mathbf{r}) + k_0^2 \int_{x_0}^{L} dx_1 \times \int G(x - x_1, \mathbf{r} - \mathbf{r}_1)\varepsilon(\mathbf{R}_1)p(x_1, \mathbf{r}_1)\, d^2 r_1. \tag{10}$$

Hereinafter, if the integration limits are not indicated, they are assumed to be from $-\infty$ to ∞. In Eq. (10), L is the right boundary of an inhomogeneous medium (for concreteness, $L > x$), $G(x, \mathbf{r})$ is the Green's function in free space,

$$G(x, \mathbf{r}) = \frac{\exp\left(ik_0\sqrt{x^2 + r^2}\right)}{4\pi\sqrt{x^2 + r^2}} = \frac{i}{8\pi^2} \int \exp\left(i\boldsymbol{\kappa} \cdot \boldsymbol{r} + i|x|\sqrt{k_0^2 - \kappa^2}\right) \frac{d^2\kappa}{\sqrt{k_0^2 - \kappa^2}}, \tag{11}$$

and $p_0(x, \mathbf{r})$ is the sound field propagating in the medium without scattering. This sound field can be readily expressed in terms of the Fourier transform $\check{p}(x_0, \boldsymbol{\kappa})$ of the sound field $p(x_0, \mathbf{r})$ incident on the medium,

$$p_0(x, \mathbf{r}) = \int \exp\left[i\boldsymbol{\kappa} \cdot \mathbf{r} + i(x - x_0)\sqrt{k_0^2 - \kappa^2}\right] \check{p}(x_0, \boldsymbol{\kappa})\, d^2\kappa. \tag{12}$$

In this paper, we use the following Fourier transform pair:

$$p(x, \mathbf{r}) = \mathcal{F}^{-1}\{\check{p}(x, \boldsymbol{\kappa})\} = \int \exp(i\boldsymbol{\kappa} \cdot \mathbf{r})\check{p}(x, \boldsymbol{\kappa})\, d^2\kappa, \tag{13}$$

$$\check{p}(x, \boldsymbol{\kappa}) = \mathcal{F}\{p(x, \mathbf{r})\} = \frac{1}{4\pi^2} \int \exp(-i\boldsymbol{\kappa} \cdot \mathbf{r})p(x, \mathbf{r})\, d^2 r, \tag{14}$$

where the integral operators $\mathcal{F}$ and $\mathcal{F}^{-1}$ denote the forward and inverse Fourier transforms, respectively.

Equation (10) can be solved iteratively, resulting in a Born series for the sound pressure

$$p(x, \mathbf{r}) = p_0(x, \mathbf{r}) + k_0^2 \int_{x_0}^{L} dx_1 \times \int G(x - x_1, \mathbf{r} - \mathbf{r}_1)\varepsilon(\mathbf{R}_1)p_0(x_1, \mathbf{r}_1)\, d^2 r_1 + k_0^4 \int_{x_0}^{L} dx_1 \int d^2 r_1\, G(x - x_1, \mathbf{r} - \mathbf{r}_1)\varepsilon(\mathbf{R}_1) \int_{x_0}^{L} dx_2 \times \int d^2 r_2\, G(x_1 - x_2, \mathbf{r}_1 - \mathbf{r}_2)\varepsilon(\mathbf{R}_2)p_0(x_2, \mathbf{r}_2) + \cdots. \tag{15}$$

Equations (10)–(15) are well known in the literature and set the stage for deriving EWAPE1.

The EWAPE1 is an equation for the sum of all multiply scattered forward waves. The first term in this sum is the field $p_0(x,\mathbf{r})$, which propagates from the plane $x_0 = \text{const}$ to the plane $x = \text{const}$ without scattering. This field is schematically shown as the diagram 1 in Fig. 1.

In the second term on the right-hand side of the Born series, Eq. (15), the Green's function is expressed as

$$G(x-x_1,\mathbf{r}-\mathbf{r}_1) = H(x-x_1)G(x-x_1,\mathbf{r}-\mathbf{r}_1) + \tilde{H}(x-x_1)G(x-x_1,\mathbf{r}-\mathbf{r}_1). \tag{16}$$

Here, $H(x)$ is the Heaviside step function and $\tilde{H}(x) = [1 - H(x)]$. On the right-hand side of Eq. (16), the first term, proportional to $H(x - x_1)$, corresponds to sound waves scattered forward (i.e., in the positive direction of the x axis) for which $x > x_1$. The second term, proportional to $\tilde{H}(x - x_1)$, corresponds to sound waves scattered backwards (i.e., in the negative direction of the x axis) for which $x < x_1$. Substitution of Eq. (16) into the second term of the Born series results in two terms which contain $H(x - x_1)$ and $\tilde{H}(x - x_1)$, respectively. The former describes the sound field singly scattered in the forward direction and is depicted as diagram 2 in Fig. 1; the latter describes the field singly scattered backwards (diagram 3).

In the third term of the Born series, the two Green's functions are expressed similarly to Eq. (16). The third term is then a sum of four terms. One of these terms contains the functions $H(x - x_1)$ and $H(x_1 - x_2)$ and corresponds to the field scattered twice forward. This field is shown as diagram 4 in Fig. 1. The term containing the functions $\tilde{H}(x - x_1)$ and $H(x_1 - x_2)$ is first scattered forward and then backwards (diagram 5). The remaining two terms also exhibit backscattering.

Equation (16) is substituted in all other terms of the Born series and the waves scattered forward are separated from those having at least one backscattering. It can be shown that the sum of all multiply scattered forward waves (diagrams 1, 2, 4, etc. in Fig. 1) satisfies the following integral equation:[17,18,23]

$$p(x,\mathbf{r}) = p_0(x,\mathbf{r}) + k_0^2 \int_{x_0}^{x} dx_1 \times \int G(x-x_1,\mathbf{r}-\mathbf{r}_1)\varepsilon(\mathbf{R}_1)p(x_1,\mathbf{r}_1)\,d^2r_1. \tag{17}$$

This equation is called the EWAPE1. It differs from the Helmholtz equation written in the integral form, Eq. (10), only by the upper limit of integration with respect to x_1; in Eq. (17) this limit coincides with the argument x of the sound pressure $p(x, \mathbf{r})$, while in Eq. (10), it is the right boundary of the medium.

The EWAPE1, Eq. (17), accounts for all waves scattered forward and therefore, is applicable for a wider range of the propagation angles θ than WAPEs used in the literature. It is valid for relatively small ε when the Born series converges. The EWAPE1 has been mainly employed for analytical studies of the statistical characteristics of electromagnetic waves in random media (e.g., see Ref. 23 and references therein). It was also used to justify the PE.[14] In Sec. IV, a split-step spectral algorithm for a numerical solution of this equation is devised.

B. Operator form of EWAPE1

Although EWAPE1 and the WAPEs describe wide-angle propagation, they have different forms and are derived by differing approaches. In this subsection, it is demonstrated that EWAPE1 can be written in an operator form and obtained by an approach similar to that for WAPEs.

Let us differentiate both sides of Eq. (17) with respect to x,

$$\frac{\partial p(x,\mathbf{r})}{\partial x} = \frac{\partial p_0(x,\mathbf{r})}{\partial x} + k_0^2 \int_{x_0}^{x} dx_1 \int \frac{\partial G(x-x_1,\mathbf{r}-\mathbf{r}_1)}{\partial x} \times \varepsilon(\mathbf{R}_1)p(x_1,\mathbf{r}_1)\,d^2r_1 + k_0^2 \int G(0,\mathbf{r}-\mathbf{r}_1)\varepsilon(x,\mathbf{r}_1)p(x,\mathbf{r}_1)\,d^2r_1. \tag{18}$$

On the right-hand side of this equation, the last term originates from differentiation of the upper limit of the integral over x_1. Notice that

$$\frac{\partial}{\partial x}G(x,\mathbf{r}) = ik_0\sqrt{1+\hat{\mu}}\,G(x,\mathbf{r}). \tag{19}$$

This relationship is a consequence of Eq. (5), where $\varepsilon = 0$, and is also valid for the first term on the right-hand side of Eq. (18), $\partial p_0(x, \mathbf{r})/\partial x$. Factoring out the pseudo-differential operator $ik_0(1 + \hat{\mu})^{1/2}$ from the first two terms on the right-hand side of Eq. (18), the remaining sum can be recognized as $p(x, \mathbf{r})$. Thus, Eq. (18) becomes

$$\left(\frac{\partial}{\partial x} - ik_0\sqrt{1+\hat{\mu}}\right)p(x,\mathbf{r}) = k_0^2 \int G(0,\mathbf{r}-\mathbf{r}_1)\varepsilon(x,\mathbf{r}_1)p(x,\mathbf{r}_1)\,d^2r_1. \tag{20}$$

This equation can be expressed in the equivalent form

$$\left(\frac{\partial}{\partial x} - ik_0\sqrt{1+\hat{\mu}}\right)p(x,\mathbf{r}) = \frac{ik_0}{2}(1+\hat{\mu})^{-1/2}[\varepsilon(x,\mathbf{r})p(x,\mathbf{r})]. \tag{21}$$

To show equivalence of these two equations, the sound pressure is expressed as the inverse Fourier transform $p(x,\mathbf{r}) = \mathcal{F}^{-1}\{\check{p}(x,\boldsymbol{\kappa})\}$. Then, Eqs. (20) and (21) reduce to the same integro-differential equation for $\check{p}$,

$$\left(\frac{\partial}{\partial x} - i\sqrt{k_0^2-\kappa^2}\right)\check{p}(x,\boldsymbol{\kappa}) = \frac{ik_0^2}{2\sqrt{k_0^2-\kappa^2}} \int \check{\varepsilon}(x,\boldsymbol{\kappa}-\boldsymbol{\kappa}_1)\check{p}(x,\boldsymbol{\kappa}_1)\,d^2\kappa_1. \tag{22}$$

Here, $\check{\varepsilon}(x,\boldsymbol{\kappa}) = \mathcal{F}\{\varepsilon(x,\mathbf{r})\}$ is the Fourier transform of $\varepsilon(x, \mathbf{r})$.

Equation (21), the operator form of EWAPE1, is a new result. For narrow-angle propagation, the pseudo-differential

operators in this equation can be approximated as $\sqrt{1+\hat{\mu}} \approx 1+\hat{\mu}/2$ and $(1+\hat{\mu})^{-1/2} \approx 1$. With these approximations, Eq. (21) becomes the PE, Eq. (7).

Equation (21) can also be derived by the approach similar to that for WAPEs (Sec. II B). In Eq. (3), we assume that ε small in comparison with $1+\hat{\mu}$. Then, the operator $\hat{Q}$ can be approximated as

$$\hat{Q} = \sqrt{(1+\hat{\mu})\left[1+(1+\hat{\mu})^{-1}\varepsilon\right]} \approx \sqrt{1+\hat{\mu}} + (1+\hat{\mu})^{-1/2}\varepsilon/2. \tag{23}$$

Substituting this result into Eq. (5), we obtain Eq. (21). Tappert[2] also considered the case when ε is small in comparison with $1+\hat{\mu}$. However, he implemented this idea in a form different from Eq. (23) and obtained an integro-differential equation for the sound field, Eq. (3.46) in Ref. 2, which seems different from Eq. (21). Tappert also wrote: "The integral operator appearing in this equation does not appear to be susceptible to further reductions."

C. EWAPE2

The EWAPE1, Eq. (17) or Eq. (21), is valid when $|\varepsilon| \ll 1$. For some problems, it is desirable to generalize this equation to relatively large ε.

To this end, Eqs. (2) and (5) are combined to arrive at the well-known one-way wave equation

$$\left(\frac{\partial}{\partial x} - ik_0\sqrt{1+\hat{\mu}(\mathbf{r})+\varepsilon(x,\mathbf{r})}\right)p(x,\mathbf{r}) = 0. \tag{24}$$

This equation enables us to consider cases (i), (ii), and (iii) formulated in the Introduction. However, as far as we know, there are no approaches for numerical solution of this equation.

In Sec. IV C, it is suggested to solve Eq. (24) by a split-step spectral algorithm. This approach is valid only if $\varepsilon(x, \mathbf{r})$ is a slowly varying function of the transverse coordinates $\mathbf{r}$. (The characteristic scale of $\varepsilon(x, \mathbf{r})$ should be much greater than $1/k_0$.) Equation (24) with a slowly varying $\varepsilon(x, \mathbf{r})$ is termed EWAPE2. As shown in Sec. II B, EWAPE1 can be obtained from Eq. (24) by assuming that ε is small in comparison with $1+\hat{\mu}$ and keeping the first two terms in the Taylor-series expansion of the square root.

To gain insight into the ranges of applicability of the two EWAPEs, in Appendix A they are used to calculate the sound pressure from a point source in a stratified medium, where $\varepsilon(x)$ depends only on x. This problem is pertinent to an acoustic source (such as an airplane) located above the ground in a stratified atmosphere, while an observation point is on the ground, or vice versa. In this case, the x axis corresponds to the vertical coordinate pointed downward or upward. The sound pressure calculated with the two EWAPEs is then compared with that obtained with the Helmholtz equation in the high-frequency approximation. It is shown that EWAPE2 correctly predicts the phase of the sound pressure, while EWAPE1 predicts it to order ε. Neither EWAPE correctly predicts the sound-pressure amplitude. Therefore, EWAPE2 should be applied cautiously when $\varepsilon(x)$ changes significantly.

IV. SPLIT-STEP SPECTRAL ALGORITHM

In this section, a split-step spectral algorithm for solving the EWAPEs is developed. Tappert[2] used a similar split-spectral Fourier algorithm to solve the PE, and Feit and Fleck[16] employed it for a WAPE (also, see Ref. 21).

A. EWAPE1

The medium between the source and receiver is divided into many 3D slabs, each of which can be depicted as the 3D slab in Fig. 1. The sound pressure $p(x_0, \mathbf{r})$ at the left boundary of the slab is known. The goal is to calculate the sound pressure $p(x, \mathbf{r})$ at the right boundary of the slab, $x = x_0 + \Delta x = \text{const}$, where

$$\Delta x = x - x_0. \tag{25}$$

After $p(x, \mathbf{r})$ is determined, this procedure repeats in the next slab until the observation point is reached.

Within the slab shown in Fig. 1, Eq. (17) is solved in the Born approximation by replacing $p(x_1, \mathbf{r}_1)$ in the integrand with the first term on the right-hand side of this equation, $p_0(x_1, \mathbf{r}_1)$,

$$p(x,\mathbf{r}) = p_0(x,\mathbf{r}) + k_0^2\int_{x_0}^{x} dx_1 \int G(x-x_1,\mathbf{r}-\mathbf{r}_1) \times \varepsilon(\mathbf{R}_1)p_0(x_1,\mathbf{r}_1)\,d^2r_1. \tag{26}$$

Replacing $G(x-x_1, \mathbf{r}-\mathbf{r}_1)$ with Eq. (11) and $p_0(x_1, \mathbf{r}_1)$ with Eq. (12), we obtain

$$p(x,\mathbf{r}) = p_0(x,\mathbf{r}) + \frac{ik_0^2}{8\pi^2}\int_{x_0}^{x} dx_1 \int d^2r_1 \int d^2\kappa \times \int \frac{d^2\kappa_1}{\sqrt{k_0^2-\kappa_1^2}}\,\varepsilon(\mathbf{R}_1)\check{p}(x_0,\boldsymbol{\kappa}) \times \exp\left[i\boldsymbol{\kappa}\cdot\mathbf{r}_1 + i\boldsymbol{\kappa}_1\cdot(\mathbf{r}-\mathbf{r}_1) + i(x_1-x_0)\sqrt{k_0^2-\kappa^2} + i(x-x_1)\sqrt{k_0^2-\kappa_1^2}\right]. \tag{27}$$

This formula can be written in the equivalent form

$$p(x,\mathbf{r}) = p_0(x,\mathbf{r}) + i\int \exp\left[i\boldsymbol{\kappa}\cdot\mathbf{r} + i\Delta x\sqrt{k_0^2-\kappa^2}\right] \times \check{p}(x_0,\boldsymbol{\kappa})\phi(x,x_0;\mathbf{r};\boldsymbol{\kappa})\,d^2\kappa, \tag{28}$$

in which the wide-angle phase factor is introduced

$$\phi(x,x_0;\mathbf{r};\boldsymbol{\kappa}) = \frac{k_0^2}{8\pi^2}\int_{x_0}^{x} dx_1 \int d^2r_1 \int \frac{d^2\kappa_1}{\sqrt{k_0^2-\kappa_1^2}}\,\varepsilon(\mathbf{R}_1) \times \exp\left[i(\boldsymbol{\kappa}-\boldsymbol{\kappa}_1)\cdot(\mathbf{r}_1-\mathbf{r}) + i(x-x_1) \times \left(\sqrt{k_0^2-\kappa_1^2} - \sqrt{k_0^2-\kappa^2}\right)\right]. \tag{29}$$

On the right-hand side of Eq. (28), $p_0(x, \mathbf{r})$ is replaced with Eq. (12) and the two integrals are combined. Assuming that $|\phi| \ll 1$ in the resulting integral, we write $1 + i\phi = \exp(i\phi)$. The sound pressure at the right boundary of the slab takes the form

$$p(x,\mathbf{r}) = \int \exp\left[i\boldsymbol{\kappa}\cdot\mathbf{r} + i\Delta x\sqrt{k_0^2-\kappa^2} + i\phi(x,x_0;\mathbf{r};\boldsymbol{\kappa})\right] \times \check{p}(x_0,\boldsymbol{\kappa})\,d^2\kappa. \tag{30}$$

Consider the wide-angle phase factor appearing in this formula. For a small range step, in Eq. (29) the factor in the exponential $i(x-x_1)(\sqrt{k_0^2-\kappa_1^2}-\sqrt{k_0^2-\kappa^2})$ can be ignored and the integral over x_1 can be replaced with Δx. The result is

$$\phi(x,x_0;\mathbf{r};\boldsymbol{\kappa}) = \Delta x\frac{k_0^2}{8\pi^2}\int d^2r_1\int\frac{d^2\kappa_1}{\sqrt{k_0^2-\kappa_1^2}}\,\varepsilon(x_0,\mathbf{r}_1) \times \exp\left[i(\boldsymbol{\kappa}-\boldsymbol{\kappa}_1)\cdot(\mathbf{r}_1-\mathbf{r})\right]. \tag{31}$$

A necessary condition for this approximation is $\Delta x \ll l$, where l is a characteristic length scale of ε. Substituting with $\varepsilon(x,\mathbf{r}) = \mathcal{F}^{-1}\{\check{\varepsilon}(x,\boldsymbol{\kappa})\}$, the phase factor simplifies to

$$\phi(x,x_0;\mathbf{r};\boldsymbol{\kappa}) = \Delta x\frac{k_0^2}{2}\int\exp(i\boldsymbol{\kappa}_1\cdot\mathbf{r})\frac{\check{\varepsilon}(x_0,\boldsymbol{\kappa}_1)}{\sqrt{k_0^2-(\boldsymbol{\kappa}_1+\boldsymbol{\kappa})^2}}\,d^2\kappa_1. \tag{32}$$

Equations (30) and (32) allow us to recalculate the sound field from the plane $x_0 = \text{const}$ to the plane $x = \text{const}$ and constitute the split-step spectral algorithm for solving EWAPE1, Eq. (17), or Eq. (21). In this approach, two integrals need to be evaluated at each range step. This approach enables us to consider cases (i) and (ii) formulated in the Introduction.

B. High-frequency approximation

The split-step algorithm formulated in Sec. IV A simplifies significantly in the high-frequency approximation $k_0 l \gg 1$. (A similar approximation is used in Sec. 11.2.2 in Ref. 11 for a WAPE in a moving medium.) In this approximation, the characteristic scale of $\check{\varepsilon}(x_0,\boldsymbol{\kappa}_1)$ with respect to $\boldsymbol{\kappa}_1$ is $1/l$. If $k_0 l \gg 1$, in the square root in Eq. (32), $\boldsymbol{\kappa}_1$ can be set to zero. The resulting integral can be evaluated with the result

$$\phi(x,x_0;\mathbf{r};\boldsymbol{\kappa}) = \Delta x\frac{k_0^2\varepsilon(x_0,\mathbf{r})}{2\sqrt{k_0^2-\kappa^2}}. \tag{33}$$

Substituting this result into Eq. (30), we obtain

$$p(x,\mathbf{r}) = \int\exp\left[i\boldsymbol{\kappa}\cdot\mathbf{r} + i\Delta x\sqrt{k_0^2-\kappa^2} + i\Delta x\frac{k_0^2\varepsilon(x_0,\mathbf{r})}{2\sqrt{k_0^2-\kappa^2}}\right]\check{p}(x_0,\boldsymbol{\kappa})\,d^2\kappa. \tag{34}$$

This equation is one of the main results of the present paper. It expresses the split-step spectral algorithm in the high-frequency approximation and enables us to consider case (i) described in the Introduction. The ranges of applicability of Eq. (34) can be summarized as

$$|\varepsilon| \ll 1, \quad \Delta x \ll l, \quad k_0 l \gg 1. \tag{35}$$

According to Eq. (34), the sound pressure at the right boundary of the slab is a sum (an integral) of plane waves propagating at different angles θ with respect to the x axis (for which $\kappa \le k_0$) and the evanescent waves ($\kappa > k_0$). One of the plane waves is shown in Fig. 2. In the considered case $|\varepsilon| \ll 1$, this plane wave propagates in the direction of the wave vector

$$\mathbf{k}_0(\boldsymbol{\kappa}) = \left(\sqrt{k_0^2-\kappa^2},\boldsymbol{\kappa}\right) \tag{36}$$

with the components $\sqrt{k_0^2-\kappa^2}$ and $\boldsymbol{\kappa}$ along the x axis and in the transverse direction (Fig. 2). The angle θ then satisfies $\sin\theta = \kappa/k_0$. The path length traveled by this wave in the 3D slab is $L = \Delta x/\cos\theta = \Delta x k_0/\sqrt{k_0^2-\kappa^2}$. In Eq. (34), the last term in the exponential describes the phase increment due to the refractive index variations, ε, along the path of the plane wave. Using the value of L, this phase increment can be written as $k_0 L\varepsilon/2 \approx k_0 L(N-1)$, where we took into account that $\varepsilon = N^2 - 1 \approx 2(N-1)$. This phase increment coincides with the geometrical acoustics calculation along the unperturbed path. (For small variations of the refractive index, the phase increment is calculated along the unperturbed path, e.g., Sec. 3.7 in Ref. 11.)

Thus, the square roots appearing in the exponential in Eq. (34) have a clear physical meaning. The first square root corresponds to the x components of the wave vectors $\mathbf{k}_0$ of the plane waves in the spectral decomposition of the sound pressure $p(x, \mathbf{r})$. The second square root corresponds to the path lengths of these waves in the 3D slab. As will be shown in Sec. IV D, WAPEs known in the literature can be obtained by different approximations of these square roots.

A preliminary numerical implementation of Eq. (34) was considered in Ref. 24. Two-dimensional (2D) sound propagation through synthetic atmospheric turbulence was analyzed. An array of regularly spaced point sources was considered in order to avoid incorporating finite impedance boundary conditions. In Eq. (34), the integral was calculated using a composite trapezoidal rule over the region, including both propagating and evanescent waves. The integration was stable but took longer than those with the narrow-angle PE and Eq. (47) below, which corresponds to one of three terms in the GFPE[25,26] and can be termed as a free-space GFPE. The reason for that is the PE and GFPE are efficient; the GFPE uses a fast Fourier transform (FFT) for solving the inverse Fourier transform. On the other hand, a "brute-force" integration approach was used to solve Eq. (34).

This preliminary numerical implementation showed that the split-step spectral algorithm is feasible, but significant improvements are needed to make it a generally useful option. For example, this approach may be improved by

incorporating absorbing or perfectly matched layers at the boundaries of the propagation domain, which would allow the domain to be much smaller and still provide useful results. Perhaps the most important problem is associated with the fact that the phase factor $\phi(x,x_0;\mathbf{r};\boldsymbol{\kappa})$ depends on both the transverse coordinates $\mathbf{r}$ and the transverse Fourier variable $\boldsymbol{\kappa}$. Because of this fact, Eq. (34) is not an inverse Fourier transform and efficient numerical algorithms, such as the FFT, may not be used. However, the phase factor changes with $\mathbf{r}$ much more slowly than the term $\exp(i\boldsymbol{\kappa}\cdot\mathbf{r})$ does. This property might be used to speed up numerical calculations; the integral in Eq. (34) can be called a quasi-Fourier integral or a quasi-Fourier inverse transform.

1. Validation of Eq. (34)

Several approximations have been used to obtain the split-step spectral algorithm, Eq. (34), for EWAPE1. In this subsection, starting from Eq. (34) we derive EWAPE1, Eq. (21). This derivation validates the split-step algorithm and elucidates its ranges of applicability.

Applying the operator $\partial/\partial x$ to both sides of Eq. (34), we obtain

$$\frac{\partial p(x,\mathbf{r})}{\partial x} = i\int\left[\sqrt{k_0^2-\kappa^2}+\frac{k_0^2\varepsilon(x_0,\mathbf{r})}{2\sqrt{k_0^2-\kappa^2}}\right] \times\exp\left[i\boldsymbol{\kappa}\cdot\mathbf{r}+i\Delta x\left(\sqrt{k_0^2-\kappa^2}+\frac{k_0^2\varepsilon(x_0,\mathbf{r})}{2\sqrt{k_0^2-\kappa^2}}\right)\right] \times\check{p}(x_0,\boldsymbol{\kappa})\,d^2\kappa. \tag{37}$$

When deriving this formula, we took into account that $\Delta x = x - x_0$. If the derivative $\partial\varepsilon/\partial\mathbf{r}$ is relatively small, the first term in the integrand can be factored out from the integral resulting in

$$\frac{\partial p(x,\mathbf{r})}{\partial x} = i\left[k_0\sqrt{1+\hat{\mu}}+\frac{k_0}{2}(1+\hat{\mu})^{-1/2}\varepsilon(x_0,\mathbf{r})\right] \times\int\exp\left[i\boldsymbol{\kappa}\cdot\mathbf{r}+i\Delta x\left(\sqrt{k_0^2-\kappa^2} +\frac{k_0^2\varepsilon(x_0,\mathbf{r})}{2\sqrt{k_0^2-\kappa^2}}\right)\right]\check{p}(x_0,\boldsymbol{\kappa})\,d^2\kappa. \tag{38}$$

Indeed, if in this equation, we apply the pseudo-differential operator to the integrand and omit $\partial\varepsilon/\partial\mathbf{r}$, we obtain Eq. (37). It can be shown that the terms proportional to $\partial\varepsilon/\partial\mathbf{r}$ can be omitted if the second and third inequalities in Eq. (35) are valid. Note that the pseudo-differential operators $(1+\hat{\mu})^{\pm1/2}$ in Eq. (38) become the square roots $(k_0^2-\kappa^2)^{\pm1/2}/k_0^{\pm1}$ in the spectral domain, Eq. (37),

$$(1+\hat{\mu})^{\pm1/2}\leftrightarrow(k_0^2-\kappa^2)^{\pm1/2}/k_0^{\pm1}. \tag{39}$$

This relationship is used in many transformations in this paper.

In Eq. (38), the integral coincides with the integral in Eq. (34) and is equal to $p(x,\mathbf{r})$. With this replacement, Eq. (38) becomes Eq. (21). Thus, the split-step spectral algorithm, Eq. (34), is indeed equivalent to EWAPE1, Eq. (21), provided that Eq. (35) is valid.

C. EWAPE2

The EWAPE2, Eq. (24), contains $\varepsilon(x,\mathbf{r})$ in the square root, which complicates the split-step spectral algorithm. Therefore, first, we assume that ε depends only on x.

In this case, in Eq. (24), the sound pressure $p(x,\mathbf{r})$ is substituted from Eq. (13). As a result, we obtain a differential equation for the Fourier transform $\check{p}(x,\boldsymbol{\kappa})$ of the sound pressure,

$$\left(\frac{\partial}{\partial x}-i\sqrt{k_0^2(1+\varepsilon(x))-\kappa^2}\right)\check{p}(x,\boldsymbol{\kappa})=0. \tag{40}$$

Solving this equation in the 3D slab (Fig. 1), we obtain

$$\check{p}(x,\boldsymbol{\kappa})=\exp\left[i\int_{x_0}^{x}\sqrt{k_0^2(1+\varepsilon(x'))-\kappa^2}\,dx'\right]\check{p}(x_0,\boldsymbol{\kappa}). \tag{41}$$

Substituting this result into Eq. (13), we express the sound pressure at the right boundary of the 3D slab in terms of $\check{p}(x_0,\boldsymbol{\kappa})$ at the left boundary,

$$p(x,\mathbf{r})=\int\exp\left[i\boldsymbol{\kappa}\cdot\mathbf{r}+i\int_{x_0}^{x}\sqrt{k_0^2(1+\varepsilon(x'))-\kappa^2}\,dx'\right] \times\check{p}(x_0,\boldsymbol{\kappa})\,d^2\kappa. \tag{42}$$

This formula is an exact result for a stratified medium. If the slab width is relatively small, in Eq. (42), the integral can be replaced with Δx,

$$p(x,\mathbf{r})=\int\exp\left[i\boldsymbol{\kappa}\cdot\mathbf{r}+\Delta x\sqrt{k_0^2[1+\varepsilon(x_0)]-\kappa^2}\right] \times\check{p}(x_0,\boldsymbol{\kappa})\,d^2\kappa. \tag{43}$$

The plane waves in the integrand of this formula propagate in the directions of the wave vectors $\mathbf{k}=(\sqrt{k_0^2(1+\varepsilon(x_0))-\kappa^2},\boldsymbol{\kappa})$. Therefore, similarly to Eq. (34), any approximation of the square root in Eq. (43) results in an approximation of the direction of propagation of the plane waves in the spectral decomposition of $p(x,\mathbf{r})$.

Now consider the case when $\varepsilon(x,\mathbf{r})$ is a slowly varying function of $\mathbf{r}$. In this case, the split-step spectral algorithm for solution of EWAPE2 can be obtained by replacing $\varepsilon(x_0)$ in Eq. (43) with $\varepsilon(x_0,\mathbf{r})$,

$$p(x,\mathbf{r})=\int\exp\left[i\boldsymbol{\kappa}\cdot\mathbf{r}+i\Delta x\sqrt{k_0^2[1+\varepsilon(x_0,\mathbf{r})]-\kappa^2}\right] \times\check{p}(x_0,\boldsymbol{\kappa})\,d^2\kappa. \tag{44}$$

This formula expresses the split-step spectral algorithm for EWAPE2.

Although Eq. (44) has been obtained by a qualitative approach, it can be validated rigorously using the method of

Sec. IV B 1. To this end, the operator $\partial/\partial x$ is applied to both sides of Eq. (44)

$$\frac{\partial p(x,\mathbf{r})}{\partial x} = i\int \sqrt{k_0^2\left[1+\varepsilon(x_0,\mathbf{r})\right]-\kappa^2} \times \exp\left[i\boldsymbol{\kappa}\cdot\mathbf{r}+i\Delta x\sqrt{k_0^2\left[1+\varepsilon(x_0,\mathbf{r})\right]-\kappa^2}\right] \times \check{p}(x_0,\boldsymbol{\kappa})\,d^2\kappa. \quad (45)$$

Similarly to Sec. IV B 1, the derivatives $\partial\varepsilon/\partial\mathbf{r}$ can be omitted provided that the second and third inequalities in Eq. (35) are valid. In this case, the square root in the integrand of Eq. (45) can be factored out from the integral

$$\frac{\partial p(x,\mathbf{r})}{\partial x} = ik_0\sqrt{1+\varepsilon(x_0,\mathbf{r})+\hat{\mu}} \times \int \exp\left[i\boldsymbol{\kappa}\cdot\mathbf{r}+i\Delta x\sqrt{k_0^2\left[1+\varepsilon(x_0,\mathbf{r})\right]-\kappa^2}\right] \times \check{p}(x_0,\boldsymbol{\kappa})\,d^2\kappa. \quad (46)$$

It follows from Eq. (44) that the integral in this equation is equal to $p(x,\mathbf{r})$. Therefore, Eq. (46) coincides with EWAPE2, Eq. (24). This validates the split-step spectral algorithm, Eq. (44), for EWAPE2. The ranges of applicability of Eq. (44) are given by the last two inequalities in Eq. (35). Equation (44) enables us to study cases (i) and (iii) formulated in the Introduction.

If $|\varepsilon| \ll 1$, the square root in Eq. (44) can be expressed as a Taylor series with respect to ε. Keeping the first two terms in the series results in Eq. (34). Thus, both EWAPE1 and the related split-step spectral algorithm can be obtained from EWAPE2 and its split-step spectral algorithm by assuming that ε is small and approximating the corresponding square roots.

D. Comparison between EWAPEs and WAPEs

Here, we show that the WAPEs considered in Sec. II B are particular cases of the EWAPEs. The WAPEs will be obtained by approximating the square roots in Eqs. (34) and (44).

In Eq. (34), the square root in the denominator can be approximated as k_0. The result is

$$p(x,\mathbf{r}) = e^{ik_0\Delta x\varepsilon(x_0,\mathbf{r})/2}\int \exp\left(i\boldsymbol{\kappa}\cdot\mathbf{r}+i\Delta x\sqrt{k_0^2-\kappa^2}\right) \times \check{p}(x_0,\boldsymbol{\kappa})\,d^2\kappa. \quad (47)$$

In this equation, the integral corresponds to sound propagation in free space in the 3D slab (Fig. 1) without any approximations. The phase increment due to the refractive index variations is calculated along the x axis rather than the propagation path (Fig. 2). This approximation is similar to that in the PE, Eq. (7), and is valid if the propagation angle θ is less than or about 20°. A similar approximation is used in the GFPE for the direct and ground reflected waves.[9,25,26] In Sec. VI, the GFPE will be generalized to account for the wide-angle phase factor.

In Eq. (47), the remaining square root can be approximated as $k_0 - \kappa^2/(2k_0)$

$$p(x,\mathbf{r}) = e^{ik_0\Delta x\varepsilon(x_0,\mathbf{r})/2}\int \exp\left[i\boldsymbol{\kappa}\cdot\mathbf{r}+ik_0\Delta x\left(1-\frac{\kappa^2}{2k_0^2}\right)\right] \times \check{p}(x_0,\boldsymbol{\kappa})\,d^2\kappa. \quad (48)$$

In this case, sound propagation in free space is considered in the narrow-angle approximation. Equation (48) can be recognized as the split-step Fourier algorithm for the PE.[2] Applying the operator $\partial/\partial x$ to both sides of this equation, it can be reduced to Eq. (7).

In Eq. (44), the second term in the exponential can be written as $k_0\sqrt{1+\varepsilon-\kappa^2/k_0^2}$. In this formula, the square root can be approximated as a Padé (n,n) series with respect to $\varepsilon-\kappa^2/k_0^2$. As a result, we obtain

$$p(x,\mathbf{r}) = \int \exp\left\{i\boldsymbol{\kappa}\cdot\mathbf{r}+i\Delta x k_0 \times\left[1+\sum_{j=1}^{n}\frac{a_{j,n}\left(\varepsilon(x_0,\mathbf{r})-\kappa^2/k_0^2\right)}{1+b_{j,n}\left(\varepsilon(x_0,\mathbf{r})-\kappa^2/k_0^2\right)}\right]\right\} \times \check{p}(x_0,\boldsymbol{\kappa})\,d^2\kappa, \quad (49)$$

where the coefficients $a_{j,n}$ and $b_{j,n}$ are the same as in Eq. (8). Applying the operator $\partial/\partial x$ to both sides of this equation we have

$$\frac{\partial p(x,\mathbf{r})}{\partial x} = ik_0\int\left[1+\sum_{j=1}^{n}\frac{a_{j,n}\left(\varepsilon(x_0,\mathbf{r})-\kappa^2/k_0^2\right)}{1+b_{j,n}\left(\varepsilon(x_0,\mathbf{r})-\kappa^2/k_0^2\right)}\right] \times \exp\left\{i\boldsymbol{\kappa}\cdot\mathbf{r}+i\Delta x k_0 \times\left[1+\sum_{j=1}^{n}\frac{a_{j,n}\left(\varepsilon(x_0,\mathbf{r})-\kappa^2/k_0^2\right)}{1+b_{j,n}\left(\varepsilon(x_0,\mathbf{r})-\kappa^2/k_0^2\right)}\right]\right\} \times \check{p}(x_0,\boldsymbol{\kappa})\,d^2\kappa. \quad (50)$$

If the derivative $\partial\varepsilon/\partial\mathbf{r}$ can be ignored, similarly to Sec. IV B 1, the first term in the integrand can be factored out from the integral and $-\kappa^2/k_0^2$ replaced with the differential operator $\hat{\mu}$ given by Eq. (4). The resulting equation can be shown to coincide with Eq. (5), where $\hat{Q}$ is given by Eq. (8). Thus, Eq. (49) is as a split-step spectral algorithm for the WAPE based on a Padé (n,n) series expansion.

Finally, in Eq. (44), the square root can be approximated as

$$k_0\sqrt{1+\varepsilon-\kappa^2/k_0^2} \approx k_0\left(\sqrt{1-\kappa^2/k_0^2}+\sqrt{1+\varepsilon}-1\right). \quad (51)$$

The resulting equation takes the form

$$p(x,\mathbf{r}) = \exp\left[i\Delta x k_0\left(\sqrt{1+\varepsilon(x_0,\mathbf{r})}-1\right)\right] \times \int \exp\left(i\boldsymbol{\kappa}\cdot\mathbf{r}+i\Delta x\sqrt{k_0^2-\kappa^2}\right)\check{p}(x_0,\boldsymbol{\kappa})\,d^2\kappa. \quad (52)$$

Again, we apply the operator $\partial/\partial x$ to both sides of this equation and show that the result coincides with Eq. (5), where $\hat{Q}$ is given by Eq. (9).

Thus, with different approximations of the square roots in Eqs. (34) and (44), we have obtained WAPEs known in the literature. These square roots correspond to the wave vectors of the plane waves in the spectral decomposition of the sound pressure at the right boundary of the 3D slab and the path lengths of these waves. Therefore, our approach provides a clear physical interpretation of approximations pertinent to the WAPEs. Note that WAPEs are usually obtained by omitting some terms in partial differential equations, which is often difficult to interpret. The approach suggested in this paper also enables us to study of the ranges of applicability of the EWAPEs and WAPEs (Sec. V).

E. New WAPE

In Eqs. (34) and (44), new approximations for the square roots might be suggested, which would result in new WAPEs. For example, in Eq. (34), both square roots can be approximated as Padé (n,n) series. This is similar to expanding both square roots in Eq. (21) as Padé (n,n) series, which results in the new WAPE

$$\left[\frac{\partial}{\partial x} - ik_0 \quad 1 + \sum_{j=1}^{n} \frac{a_{j,n}\hat{\mu}}{1 + b_{j,n}\hat{\mu}}\right] p(x,\mathbf{r}) = \frac{ik_0}{2} \quad 1 + \sum_{j=1}^{n} \frac{\tilde{a}_{j,n}\hat{\mu}}{1 + \tilde{b}_{j,n}\hat{\mu}}\Bigg)[\varepsilon(x,\mathbf{r})p(x,\mathbf{r})]. \tag{53}$$

Here, the coefficients $a_{j,n}$ and $b_{j,n}$ are the same as in Eq. (8), while $\tilde{a}_{j,n}$ and $\tilde{b}_{j,n}$ are new coefficients that depend on n and can be determined following approaches known in the literature (e.g., Ref. 4). For example, for $n=1$, the operator $(1+\hat{\mu})^{-1/2}$ can be approximated as

$$(1+\hat{\mu})^{-1/2} = 1 + \frac{\tilde{a}_{1,1}\hat{\mu}}{1 + \tilde{b}_{1,1}\hat{\mu}}. \tag{54}$$

The coefficients $\tilde{a}_{1,1}$ and $\tilde{b}_{1,1}$ can be determined by equating the first two derivatives of the left- and right-hand sides of Eq. (54) with the result $\tilde{a}_{1,1} = -1/4$ and $\tilde{b}_{1,1} = 3/4$. In Eq. (53), ε is a small parameter. Therefore, this equation might be simpler than the WAPE, in which the operator $\hat{Q}$ is approximated by Eq. (8). In the latter equation, increasing n allows one to consider increasing values of ε, which is not needed if $|\varepsilon| \ll 1$.

V. PHASE ERRORS IN EWAPES AND WAPES

WAPEs are usually employed to recalculate the sound pressure from the left boundary of a slab to its right boundary (Fig. 1). Accuracy of different WAPEs is often assessed by the phase errors of a plane wave in a homogeneous slab (e.g., Refs. 16 and 21). In this section, we compare the phase errors pertinent to the EWAPEs and WAPEs.

A. Plane wave in a homogeneous slab

Consider a plane wave incident on the 3D slab located between the planes $x_0 = \text{const}$ and $x = x_0 + \Delta x = \text{const}$ (Fig. 1) in which $\varepsilon = \text{const}$. The Fourier transform of the sound pressure of this wave at the left boundary of the slab is

$$\check{p}_0(x_0,\boldsymbol{\kappa}) = A\delta(\boldsymbol{\kappa} - \boldsymbol{\kappa}_0). \tag{55}$$

Here, A characterizes the amplitude of the plane wave and $\boldsymbol{\kappa}_0$ its direction of propagation.

Equation (43) is an exact result for the homogeneous slab in which $\varepsilon = \text{const}$. Substituting Eq. (55) into Eq. (43), we determine the sound pressure at the right boundary of the slab

$$p(x,\mathbf{r}) = A\,\exp\left[i\boldsymbol{\kappa}_0\cdot\mathbf{r} + i\Delta x\sqrt{k_0^2(1+\varepsilon) - \kappa_0^2}\right] = A\,\exp(i\Phi). \tag{56}$$

Here, Φ is the exact phase increment of the plane wave after propagation through the slab,

$$\Phi = \boldsymbol{\kappa}_0\cdot\mathbf{r} + \Delta x\sqrt{k_0^2(1+\varepsilon) - \kappa_0^2}. \tag{57}$$

Inside the slab, the plane wave propagates as shown in Fig. 2. The propagation angle θ with respect to the x axis is determined by $\sin\theta = \kappa_0/\sqrt{k_0^2(1+\varepsilon)}$. The phase increment Φ can also be calculated using geometrical acoustics. The result $\Phi = k_0 L\sqrt{1+\varepsilon}$ coincides with Eq. (57), if we take into account that the path length of the sound wave inside the slab is $L = \Delta x/\cos\theta$.

B. Phase errors

The phase increments of the considered plane wave can also be calculated with the EWAPEs and WAPEs considered above and then compared with the exact phase increment, Eq. (57).

Substituting Eq. (55) into Eq. (34) and calculating the resulting integral, we obtain the phase increment of the plane wave at the right boundary of the slab calculated with EWAPE1,

$$\Phi_{\text{EWAPE1}} = \boldsymbol{\kappa}_0\cdot\mathbf{r} + \Delta x k_0\left(\sqrt{1-\kappa_0^2/k_0^2} + \frac{\varepsilon}{2\sqrt{1-\kappa_0^2/k_0^2}}\right). \tag{58}$$

The phase increment Φ_{EWAPE1} differs from the exact phase increment Φ in Eq. (57).

Similar to Eq. (43), Eq. (44) is also the exact result for the homogeneous slab. Therefore, the phase increment calculated with EWAPE2, Φ_{EWAPE2}, coincides with Φ from Eq. (57).

The phase increments of the plane sound wave after propagation through the 3D homogeneous slab can also be calculated with the PE and WAPEs considered in Secs. II B and IV D. For the GFPE, Eq. (47), the result is

$$\Phi_{\mathrm{GFPE}} = \boldsymbol{\kappa}_0 \cdot \mathbf{r} + \Delta x k_0 \left(\sqrt{1 - \kappa_0^2/k_0^2} + \varepsilon/2 \right). \tag{59}$$

For the PE, Eq. (48) or Eq. (7),

$$\Phi_{\mathrm{PE}} = \boldsymbol{\kappa}_0 \cdot \mathbf{r} + \Delta x k_0 \left[1 - \kappa_0^2/(2k_0^2) + \varepsilon/2 \right]. \tag{60}$$

For the Padé (n,n) approximation, Eq. (49),

$$\Phi_{\mathrm{Pade}(n,n)} = \boldsymbol{\kappa}_0 \cdot \mathbf{r} + \Delta x k_0 \left(1 + \sum_{j=1}^{n} \frac{a_{j,n}\left(\varepsilon - \kappa_0^2/k_0^2\right)}{1 + b_{j,n}\left(\varepsilon - \kappa_0^2/k_0^2\right)} \right). \tag{61}$$

Finally, for the operator splitting suggested by Feit and Fleck, Eq. (52),

$$\Phi_{\mathrm{FF}} = \boldsymbol{\kappa}_0 \cdot \mathbf{r} + \Delta x k_0 \left(\sqrt{1 - \kappa_0^2/k_0^2} + \sqrt{1+\varepsilon} - 1 \right). \tag{62}$$

Let us consider the normalized differences between the exact phase increment and those calculated using the EWAPEs and WAPEs,

$$\Delta\Phi_\alpha = \frac{\Phi - \Phi_\alpha}{\Delta x k_0}, \tag{63}$$

where the subscript α stands for EWAPE1, EWAPE2, GFPE, PE, Padé (n,n), and FF. These normalized phase differences indicate the phase errors pertinent to different equations. They are plotted in Figs. 3 and 4 versus the angle θ_0, defined as $\sin\theta_0 = \kappa_0/k_0$. The results for the Padé (1,1) approximation (with $a_{1,1} = 1/2$ and $b_{1,1} = 1/4$) and Padé (2,2) approximation (with the coefficients $a_{j,2}$ and $b_{j,2}$ from Ref. 5) are plotted. Only the phase errors $|\Delta\Phi_\alpha| \le 0.05$ are depicted. In Fig. 3, $\varepsilon = 0.01$. For sound

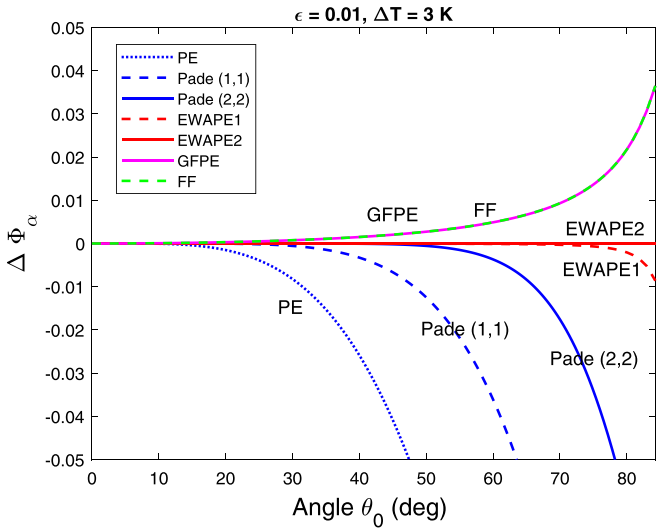

FIG. 3. (Color online) Normalized differences between the exact phase increment of a plane wave after propagation through the 3D homogeneous slab with $\varepsilon = 0.01$ and those calculated with the EWAPEs and WAPEs versus the angle θ_0.

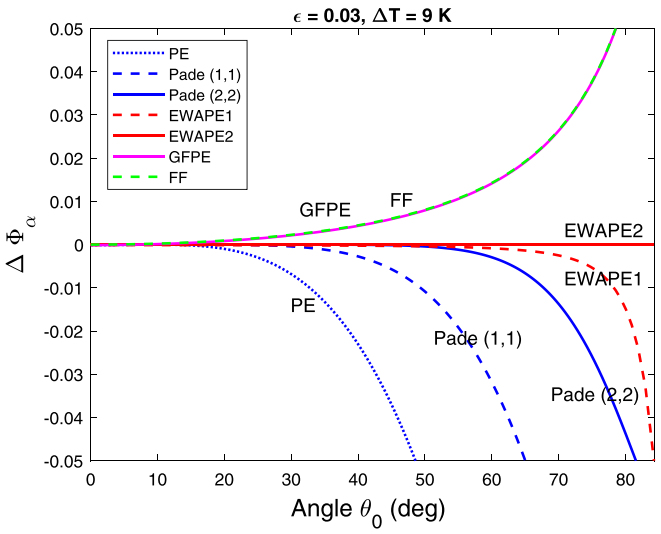

FIG. 4. (Color online) The same as in Fig. 3 but for $\varepsilon = 0.03$.

propagation in the atmosphere, $\varepsilon = 0.01$ corresponds to the temperature variation $\Delta T = 3$ K; see a paragraph above Eq. (85). As noted above, the phase error for EWAPE2, Eq. (44), is zero. Among other formulations, EWAPE1, Eq. (34), has the smallest error, followed by the Padé (2,2) approximation, the Feit and Fleck approximation, which almost coincides with the GFPE, the Padé (1,1) approximation, and finally, the PE.

In Fig. 4, the refractive index variation is larger, $\varepsilon = 0.03$ and $\Delta T = 9$ K. The results, however, are similar to Fig. 3 except that the Padé (1,1) approximation is more accurate than the GFPE and the Feit and Fleck approximation.

These numerical results show that, aside from EWAPE2, Eq. (34) has a wider range of applicability with respect to the propagation angle. Therefore, although it might be computationally intensive, this equation might be used when other equations do not provide the desired accuracy. For the homogeneous slab, the split-step spectral algorithm, Eq. (44), for EWAPE2 does not have any phase errors. However, we should recall that this equation is valid only if $\varepsilon(x, \mathbf{r})$ varies slowly with respect to $\mathbf{r}$.

VI. EXTRA-WIDE-ANGLE GFPE

In atmospheric acoustics, interaction of sound waves with the ground is usually important. This interaction can be accounted for using the GFPE, e.g., Refs. 9, 25, and 26. As indicated above, in the current version of the GFPE, the phase factor due to the refractive index variations is formulated in the narrow-angle approximation. In this section, we provide the GFPE with the wide-angle phase factor. To simplify formulations, we will consider 2D sound propagation. This will also enable us to establish a connection between the 3D and 2D WAPEs. (The other sections so far dealt with 3D sound propagation.)

Based on Sec. IV and Eq. (H.40) in Ref. 9, in a motionless medium, the GFPE with the wide-angle phase factor can be written as

$$p(x,z)=\int_{-\infty}^{\infty}\exp\left(i\kappa z+i\Delta x\sqrt{k_0^2(1+\varepsilon(x_0,z))-\kappa^2}\right)\times\left[\check{p}(x_0,\kappa)+\mathcal{R}(\kappa)\check{p}(x_0,-\kappa)\right]d\kappa+i4\pi k_s\check{p}(x_0,k_s)\times\exp\left(-ik_sz+i\Delta x\sqrt{k_0^2(1+\varepsilon(x_0,z))-k_s^2}\right).\quad(64)$$

Here, z is the transverse coordinate, $\mathcal{R}=(\kappa Z_g-k_0)/(\kappa Z_g+k_0)$ is the plane-wave reflection coefficient, Z_g is the ground impedance, $k_s=k_0/Z_g$ is the complex wavenumber pertinent to a surface wave, and

$$\check{p}(x,\kappa)=\frac{1}{2\pi}\int_0^{\infty}\exp(-i\kappa z)p(x,z)\,dz.\quad(65)$$

The three terms on the right-hand side of Eq. (64) correspond to the direct, ground reflected, and surface waves. If $\varepsilon=0$ (i.e., sound propagates in a homogeneous atmosphere above an impedance ground), this equation is an exact result and coincides with Eq. (H.40) in Ref. 9. If $\varepsilon=$const, Eq. (64) is still an exact result and can be obtained from Eq. (H.40) by writing the reference wave number as $k_0\sqrt{1+\varepsilon}$. In an inhomogeneous medium, Eq. (64) describes sound propagation approximately and is valid if $\varepsilon(x,z)$ is a slowly varying function of z.

Assuming that $|\varepsilon|\ll 1$, in Eq. (64), the square root $\sqrt{k_0^2(1+\varepsilon)-\kappa^2}$ can be approximated with the first two terms in the Taylor series with respect to ε. The result is

$$p(x,z)=\int_{-\infty}^{\infty}\exp\left[i\kappa z+i\Delta x\left(\sqrt{k_0^2-\kappa^2}+\frac{k_0^2\varepsilon(x_0,z)}{2\sqrt{k_0^2-\kappa^2}}\right)\right]\times\left[\check{p}(x_0,\kappa)+\mathcal{R}(\kappa)\check{p}(x_0,-\kappa)\right]d\kappa+i4\pi k_s\check{p}(x_0,k_s)\times\exp\left[-ik_sz+i\Delta x\left(\sqrt{k_0^2-k_s^2}+\frac{k_0^2\varepsilon(x_0,z)}{2\sqrt{k_0^2-k_s^2}}\right)\right].\quad(66)$$

Equations (64) and (66) are new results. They present the GFPEs with the wide-angle phase factors and can be termed extra-wide-angle GFPEs. If $\mathcal{R}=0$ and $k_s=0$, Eqs. (64) and (66) coincide with 2D versions of Eqs. (44) and (34), respectively, which have been derived by rigorous approaches. This provides additional justification for the extra-wide-angle GFPEs. This also elucidates how results for 3D propagation can be applied to the 2D case: the vectors $\mathbf{r}$ and $\boldsymbol{\kappa}$ should be replaced with z and κ, respectively. Numerical implementation of Eq. (66) is similar to that of Eq. (34).

The extra-wide-angle GFPEs also enable us to better understand approximations involved in the narrow-angle GFPE. In Eq. (66), approximating the square roots in the dominators as k_0, we obtain

$$p(x,z)=e^{i\Delta xk_0\varepsilon(x_0,z)/2}\left\{\int_{-\infty}^{\infty}\exp\left(i\kappa z+i\Delta x\sqrt{k_0^2-\kappa^2}\right)\times\left[\check{p}(x_0,\kappa)+\mathcal{R}(\kappa)\check{p}(x_0,-\kappa)\right]d\kappa+i4\pi k_s\check{p}(x_0,k_s)\times\exp\left(-ik_sz+i\Delta x\sqrt{k_0^2-k_s^2}\right)\right\}.\quad(67)$$

This equation coincides with the GFPE used in the literature, e.g., Eq. (H.49) in Ref. 9. To derive this equation, the wide-angle phase factor in Eq. (66) was replaced with the narrow-angle phase factor, $\exp(i\Delta xk_0\varepsilon/2)$, which is valid for the propagation angles $|\theta|\lesssim 20^\circ$.

VII. MOVING MEDIUM

In this section, the results are generalized to a moving medium with variable density. The formulation of the problem coincides with that in Sec. II A, except that the medium is moving with velocity $\mathbf{v}=(v_1,v_2,v_3)=(v_x,v_y,v_z)$ and the density ϱ is not constant. The sound pressure satisfies Eq. (1) if ε is replaced with the differential operator [Eq. (6.91) in Ref. 11]

$$\hat{\mathcal{E}}=\varepsilon-\left(\frac{\nabla\varrho}{\varrho}\right)\cdot\left(\frac{\nabla}{k_0^2}\right)+\frac{2i}{k_0^2}\left[\frac{k_0}{c_0}(\mathbf{v}\cdot\nabla)-\frac{1}{\omega}\sum_{i,j=1}^{3}\frac{\partial v_i}{\partial x_j}\frac{\partial^2}{\partial x_i\partial x_j}\right].\quad(68)$$

Here, $(x_1,x_2,x_3)=(x,y,z)$. Equation (68) is valid to order v/c_0, which is a small parameter. The operator $\hat{\mathcal{E}}$ can be generalized to account for the case $v/c_0\sim 1$.[8,10,27]

Many equations from Secs. III and IV, which contain $\varepsilon(\mathbf{R})$, are valid for a moving medium with the following substitution:

$$\varepsilon(\mathbf{R})\to\hat{\mathcal{E}}(\mathbf{R}).\quad(69)$$

For example, this substitution can be employed in a Padé (n,n) approximation for the operator $\hat{Q}$, Eq. (8), or in EWAPE1, Eq. (21). The resulting equations are, however, rather complicated since they contain many derivatives of the sound pressure and medium velocity, e.g., Refs. 7, 8, and 27 and Sec. 2.5.3 in Ref. 11. In this section, Eq. (69) is used in the split-step spectral algorithm for EWAPE1, which enables us to replace these derivatives with the wave vectors in the spectral domain. After the algorithm is generalized to a moving medium, it is possible to derive the corresponding EWAPE (Sec. VII D).

A. Split-step spectral algorithm

Employing the substitution, Eq. (69), in Eq. (26) and replacing p_0 in the integrand with Eq. (12), we obtain

$$p(x,\mathbf{r})=p_0(x,\mathbf{r})+k_0^2\int_{x_0}^{x}dx_1\int d^2r_1\times\int d^2\kappa\,G(x-x_1,\mathbf{r}-\mathbf{r}_1)\check{p}(x_0,\boldsymbol{\kappa})\times\hat{\mathcal{E}}(\mathbf{R}_1)\exp\left[i\boldsymbol{\kappa}\cdot\mathbf{r}_1+i(x_1-x_0)\sqrt{k_0^2-\kappa^2}\right].\quad(70)$$

Consider the application of the operator $\hat{\mathcal{E}}(\mathbf{R}_1)$ to the exponential function in the preceding equation. In this operator, the density can be written as $\varrho=\varrho_0+\tilde{\varrho}$, where ϱ_0 is the

reference density, which is constant, and $\tilde{\varrho}$ is the density variation. Then, in Eq. (68), $\nabla\varrho/\varrho \approx \nabla\tilde{\varrho}/\varrho_0$. The exponential function in Eq. (70) can be written $\exp(i\mathbf{k}_0(\boldsymbol{\kappa})\cdot\mathbf{R}_1 - ix_0\sqrt{k_0^2-\kappa^2})$. Here, $\mathbf{k}_0(\boldsymbol{\kappa})$ is the wave vector of the plane wave incident on a medium inhomogeneity located at the point $\mathbf{R}_1$. This wave vector is given by Eq. (36) and shown in Fig. 1. With these notations, the application of the operator $\hat{\mathcal{E}}(\mathbf{R}_1)$ to the exponential function in Eq. (70) can be readily evaluated resulting in

$$\hat{\mathcal{E}}(\mathbf{R}_1)\exp(i\mathbf{k}_0(\boldsymbol{\kappa})\cdot\mathbf{R}_1 - ix_0\sqrt{k_0^2-\kappa^2}) = \mathcal{E}(\mathbf{R}_1;\boldsymbol{\kappa})\exp\left[i\boldsymbol{\kappa}\cdot\mathbf{r}_1 + i(x_1-x_0)\sqrt{k_0^2-\kappa^2}\right]. \quad (71)$$

On the right-hand side of this formula, we substituted with the value of $\mathbf{k}_0$. In Eq. (71), the function $\mathcal{E}(\mathbf{R}_1;\boldsymbol{\kappa})$ is given by

$$\mathcal{E}(\mathbf{R}_1;\boldsymbol{\kappa}) = \varepsilon(\mathbf{R}_1) - \frac{i}{\varrho_0 k_0^2}\,\mathbf{k}_0\cdot\nabla_1\tilde{\varrho}(\mathbf{R}_1) - \frac{2}{\omega}\,\mathbf{k}_0\cdot\mathbf{v}(\mathbf{R}_1) + \frac{2i}{\omega k_0^2}\sum_{i,j=1}^{3} k_{0,i}k_{0,j}\frac{\partial v_i(\mathbf{R}_1)}{\partial x_j}, \quad (72)$$

where $\nabla_1 = \partial/\partial\mathbf{R}_1$, and x_i and $k_{0,i}$ are the components of the vectors $\mathbf{R}_1$ and $\mathbf{k}_0$. In Eq. (72), the sum can be written as $(\mathbf{k}_0\cdot\nabla_1)(\mathbf{k}_0\cdot\mathbf{v}(\mathbf{R}_1))$, leading to the form

$$\mathcal{E}(\mathbf{R}_1;\boldsymbol{\kappa}) = \varepsilon(\mathbf{R}_1) - \frac{i}{\varrho_0 k_0^2}\,\mathbf{k}_0\cdot\nabla_1\tilde{\varrho}(\mathbf{R}_1) - \frac{2}{\omega}\,\mathbf{k}_0\cdot\mathbf{v}(\mathbf{R}_1) + \frac{2i}{\omega k_0^2}(\mathbf{k}_0\cdot\nabla_1)(\mathbf{k}_0\cdot\mathbf{v}(\mathbf{R}_1)). \quad (73)$$

Next we substitute Eq. (71) into Eq. (70), and replace the Green's function with its spectral form given in Eq. (11) to obtain

$$p(x,\mathbf{r}) = p_0(x,\mathbf{r}) + \frac{ik_0^2}{8\pi^2}\int_{x_0}^{x} dx_1\int d^2r_1\int d^2\kappa \times\int\frac{d^2\kappa_1}{\sqrt{k_0^2-\kappa_1^2}}\,\mathcal{E}(\mathbf{R}_1;\boldsymbol{\kappa})\check{p}(x_0,\boldsymbol{\kappa}) \times\exp\Big[i\boldsymbol{\kappa}\cdot\mathbf{r}_1 + i\boldsymbol{\kappa}_1\cdot(\mathbf{r}-\mathbf{r}_1) + i(x_1-x_0) \times\sqrt{k_0^2-\kappa^2} + i(x-x_1)\sqrt{k_0^2-\kappa_1^2}\Big]. \quad (74)$$

This formula can be written in an equivalent form, namely

$$p(x,\mathbf{r}) = p_0(x,\mathbf{r}) + i\int\exp\left[i\boldsymbol{\kappa}\cdot\mathbf{r} + i\Delta x\sqrt{k_0^2-\kappa^2}\right] \times\check{p}(x_0,\boldsymbol{\kappa})\phi(x,x_0;\mathbf{r};\boldsymbol{\kappa})\,d^2\kappa, \quad (75)$$

in which we have introduced the wide-angle phase factor for a moving medium

$$\phi(x,x_0;\mathbf{r};\boldsymbol{\kappa}) = \frac{k_0^2}{8\pi^2}\int_{x_0}^{x} dx_1\int d^2r_1\int\frac{d^2\kappa_1}{\sqrt{k_0^2-\kappa_1^2}}\,\mathcal{E}(\mathbf{R}_1;\boldsymbol{\kappa}) \times\exp\Big[i(\boldsymbol{\kappa}-\boldsymbol{\kappa}_1)\cdot(\mathbf{r}_1-\mathbf{r}) + i(x-x_1)\left(\sqrt{k_0^2-\kappa_1^2}-\sqrt{k_0^2-\kappa^2}\right)\Big]. \quad (76)$$

Equation (75) has the same form as Eq. (28) and can be written as Eq. (30), which is repeated here for convenience

$$p(x,\mathbf{r}) = \int\exp\left[i\boldsymbol{\kappa}\cdot\mathbf{r} + i\Delta x\sqrt{k_0^2-\kappa^2} + i\phi(x,x_0;\mathbf{r};\boldsymbol{\kappa})\right] \times\check{p}(x_0,\boldsymbol{\kappa})\,d^2\kappa. \quad (77)$$

Thus, the split-step spectral algorithm for the EWAPE in a moving medium has the same form as in a motionless medium, but with a different phase factor. The wide-angle phase factor ϕ for a moving medium is evaluated in Sec. VII B.

B. Phase factor

In Eq. (76), the function $\mathcal{E}$ contains the spatial derivatives $\partial/\partial\mathbf{R}_1$ of the density and velocity. These derivatives can be eliminated from the integrals over x_1 and $\mathbf{r}_1$ similarly to sound scattering by atmospheric turbulence (e.g., Sec. 6.4.2 in Ref. 11). As shown in Appendix B, the differential operator in Eq. (73) can be replaced with the following vector:

$$\nabla_1 \to i[\mathbf{k}_0(\boldsymbol{\kappa}_1) - \mathbf{k}_0(\boldsymbol{\kappa})]. \quad (78)$$

Here, $\mathbf{k}_0(\boldsymbol{\kappa}_1)$ is the wave vector of the scattered wave shown in Fig. 1. With this substitution, the function $\mathcal{E}$ takes the form

$$\mathcal{E}(\mathbf{R}_1;\boldsymbol{\kappa},\boldsymbol{\kappa}_1) = \varepsilon(\mathbf{R}_1) - \left[1 - \frac{\mathbf{k}_0(\boldsymbol{\kappa})\cdot\mathbf{k}_0(\boldsymbol{\kappa}_1)}{k_0^2}\right]\frac{\tilde{\varrho}(\mathbf{R}_1)}{\varrho_0} - 2\frac{\mathbf{k}_0(\boldsymbol{\kappa})\cdot\mathbf{k}_0(\boldsymbol{\kappa}_1)}{k_0^2}\,\frac{\mathbf{k}_0(\boldsymbol{\kappa})\cdot\mathbf{v}(\mathbf{R}_1)}{k_0 c_0}. \quad (79)$$

Here, due to Eq. (78), the function $\mathcal{E}$ has an additional argument $\boldsymbol{\kappa}_1$, and the two velocity terms appearing in Eq. (73) are combined. Note that Eq. (73) contains imaginary terms, which become real functions in Eq. (79). From a physics point of view, all terms in the function $\mathcal{E}$ should be real since the phase factor must be a real function. (The evanescent waves with $\kappa > k_0$ should be considered separately.)

Let us introduce the unit vectors in the directions of the wave vectors $\mathbf{k}_0(\boldsymbol{\kappa})$ and $\mathbf{k}_0(\boldsymbol{\kappa}_1)$ shown in Fig. 1: $\mathbf{s}(\boldsymbol{\kappa}) = \mathbf{k}_0(\boldsymbol{\kappa})/k_0$ and $\mathbf{s}(\boldsymbol{\kappa}_1) = \mathbf{k}_0(\boldsymbol{\kappa}_1)/k_0$. With these notations, Eq. (79) takes the form

$$\mathcal{E}(\mathbf{R}_1;\boldsymbol{\kappa},\boldsymbol{\kappa}_1) = \varepsilon(\mathbf{R}_1) - \big[1 - \mathbf{s}(\boldsymbol{\kappa})\cdot\mathbf{s}(\boldsymbol{\kappa}_1)\big]\frac{\tilde{\varrho}(\mathbf{R}_1)}{\varrho_0} - 2\big[\mathbf{s}(\boldsymbol{\kappa})\cdot\mathbf{s}(\boldsymbol{\kappa}_1)\big]\big[\mathbf{s}(\boldsymbol{\kappa})\cdot\mathbf{v}(\mathbf{R}_1)/c_0\big]. \quad (80)$$

This formula describes the radiation patterns of sound scattering at the point $\mathbf{R}_1$ inside the slab, with $\mathbf{s}(\boldsymbol{\kappa})$ and $\mathbf{s}(\boldsymbol{\kappa}_1)$

being the directions of the incident and scattered waves, respectively. These radiation patterns coincide with those of a sound wave scattered by the sound speed, density, and velocity fluctuations known in the literature, e.g., see Eq. (6.100) in Ref. 11. Note that in Eq. (80), the components of the vectors $\mathbf{s}(\boldsymbol{\kappa})$ and $\mathbf{s}(\boldsymbol{\kappa}_1)$ in the direction of the x axis are positive, while similar vectors in Ref. 11 have arbitrary directions.

Equation (80) is next substituted into Eq. (76). For a small range step, the factor $i(x-x_1)(\sqrt{k_0^2-\kappa_1^2}-\sqrt{k_0^2-\kappa^2})$ in the exponential can be omitted and the integral over x_1 can be replaced with Δx. The result is

$$\phi(x,x_0;\mathbf{r};\boldsymbol{\kappa}) = \Delta x \frac{k_0^2}{8\pi^2}\int d^2r_1 \int d^2\kappa_1 \times \exp\left[i(\boldsymbol{\kappa}-\boldsymbol{\kappa}_1)\cdot(\mathbf{r}_1-\mathbf{r})\right]\frac{\mathcal{E}(x_0,\mathbf{r}_1;\boldsymbol{\kappa},\boldsymbol{\kappa}_1)}{\sqrt{k_0^2-\kappa_1^2}}. \tag{81}$$

Let

$$\check{\varepsilon}(x,\boldsymbol{\kappa}) = \mathcal{F}\{\varepsilon(x,\mathbf{r})\},\quad \check{\varrho}(x,\boldsymbol{\kappa}) = \mathcal{F}\{\tilde{\varrho}(x,\mathbf{r})\},\quad \check{\mathbf{v}}(x,\boldsymbol{\kappa}) = \mathcal{F}\{\mathbf{v}(x,\mathbf{r})\}, \tag{82}$$

be the Fourier transforms of the corresponding quantities. Then, the phase factor simplifies to

$$\phi(x,x_0;\mathbf{r};\boldsymbol{\kappa}) = \Delta x \frac{k_0^2}{2}\int \exp(i\boldsymbol{\kappa}_1\cdot\mathbf{r})\frac{\check{\mathcal{E}}(x_0;\boldsymbol{\kappa},\boldsymbol{\kappa}_1)}{\sqrt{k_0^2-(\boldsymbol{\kappa}_1+\boldsymbol{\kappa})^2}}d^2\kappa_1, \tag{83}$$

where function $\check{\mathcal{E}}$ is given by

$$\check{\mathcal{E}}(x_0;\boldsymbol{\kappa},\boldsymbol{\kappa}_1) = \check{\varepsilon}(x_0,\boldsymbol{\kappa}_1) - \left[1-\mathbf{s}(\boldsymbol{\kappa})\cdot\mathbf{s}(\boldsymbol{\kappa}_1+\boldsymbol{\kappa})\right]\times\frac{\check{\varrho}(x_0,\boldsymbol{\kappa}_1)}{\varrho_0} - 2\left[\mathbf{s}(\boldsymbol{\kappa})\cdot\mathbf{s}(\boldsymbol{\kappa}_1+\boldsymbol{\kappa})\right]\times\left[\mathbf{s}(\boldsymbol{\kappa})\cdot\check{\mathbf{v}}(x_0,\boldsymbol{\kappa}_1)/c_0\right]. \tag{84}$$

Thus, the split-step spectral algorithm for the EWAPE in a moving medium is given by Eqs. (77) and (83). This approach enables us to study cases (i) and (ii) formulated in the Introduction. Complicated derivatives of the sound pressure, medium velocity, and density appearing in the operator $\hat{\mathcal{E}}$ are replaced in Eq. (84) with the unit vectors $\mathbf{s}(\boldsymbol{\kappa})$ and $\mathbf{s}(\boldsymbol{\kappa}_1)$ in the directions of the incident and scattered waves.

The sound speed can be written as $c = c_0 + \tilde{c}$, where $\tilde{c}$ is the sound speed variation. If $|\tilde{c}/c_0| \ll 1$, then $\varepsilon = -2\tilde{c}/c_0$. We use Eq. (8.56) in Ref. 11 to write $2\tilde{c}/c_0 = \beta_c\tilde{T}/T_0$ and similarly, $\tilde{\varrho}/\varrho_0 = \beta_\varrho\tilde{T}/T_0$. Here, T_0 is the reference temperature and $\tilde{T}$ is the temperature variation. In the atmosphere, $\beta_c = 1$ and $\beta_\varrho = -1$. With these substitutions, Eq. (84) expresses the function $\check{\mathcal{E}}$ in terms of the temperature and medium velocity

$$\check{\mathcal{E}}(x_0;\boldsymbol{\kappa},\boldsymbol{\kappa}_1) = -\mathbf{s}(\boldsymbol{\kappa})\cdot\mathbf{s}(\boldsymbol{\kappa}_1+\boldsymbol{\kappa})\frac{\check{T}(x_0,\boldsymbol{\kappa}_1)}{T_0} - 2\left[\mathbf{s}(\boldsymbol{\kappa})\cdot\mathbf{s}(\boldsymbol{\kappa}_1+\boldsymbol{\kappa})\right]\left[\mathbf{s}(\boldsymbol{\kappa})\cdot\check{\mathbf{v}}(x_0,\boldsymbol{\kappa}_1)/c_0\right]. \tag{85}$$

Here, $\check{T}(x,\boldsymbol{\kappa}) = \mathcal{F}\{\tilde{T}(x,\mathbf{r})\}$.

C. High-frequency approximation

Let $k_0 l \gg 1$, where l is a characteristic length scale of ε, ϱ, or $\mathbf{v}$. Then, the characteristic scale of $\check{\varepsilon}(x_0,\boldsymbol{\kappa}_1)$, $\check{\varrho}(x_0,\boldsymbol{\kappa}_1)$, and $\check{\mathbf{v}}(x_0,\boldsymbol{\kappa}_1)$ with respect to $\boldsymbol{\kappa}_1$ is $1/l$, which is much smaller than k_0. In this case, in Eq. (84), we can set $\mathbf{s}(\boldsymbol{\kappa}_1+\boldsymbol{\kappa}) \approx \mathbf{s}(\boldsymbol{\kappa})$. This equation simplifies to

$$\check{\mathcal{E}}(x_0;\boldsymbol{\kappa},\boldsymbol{\kappa}_1) = \check{\varepsilon}(x_0,\boldsymbol{\kappa}_1) - 2[\mathbf{s}(\boldsymbol{\kappa})\cdot\check{\mathbf{v}}(x_0,\boldsymbol{\kappa}_1)/c_0]. \tag{86}$$

This result is substituted into Eq. (83). In the square root of the resulting equation, $\boldsymbol{\kappa}_1$ can be set to zero; this approximation is similar to $\mathbf{s}(\boldsymbol{\kappa}_1+\boldsymbol{\kappa}) \approx \mathbf{s}(\boldsymbol{\kappa})$. With this approximation, the integral over $\boldsymbol{\kappa}_1$ can be calculated

$$\phi(x,x_0;\mathbf{r};\boldsymbol{\kappa}) = \Delta x k_0^2 \frac{\varepsilon(x_0,\mathbf{r}) - 2\mathbf{s}(\boldsymbol{\kappa})\cdot\mathbf{v}(x_0,\mathbf{r})/c_0}{2\sqrt{k_0^2-\kappa^2}}. \tag{87}$$

This result generalizes the phase factor given by Eq. (33) to a moving medium. When $k_0 l \gg 1$, scattering primarily occurs in the direction of sound propagation, which is characterized by the vector $\mathbf{s}(\boldsymbol{\kappa})$. As a result, the density term is not present in Eq. (87), and only projection of the wind velocity on the direction of propagation appears in this equation. Substituting Eq. (87) into Eq. (77), we have

$$p(x,\mathbf{r}) = \int \exp\left[i\boldsymbol{\kappa}\cdot\mathbf{r} + i\Delta x\sqrt{k_0^2-\kappa^2} + i\Delta x k_0^2\frac{\varepsilon(x_0,\mathbf{r}) - 2\mathbf{s}(\boldsymbol{\kappa})\cdot\mathbf{v}(x_0,\mathbf{r})/c_0}{2\sqrt{k_0^2-\kappa^2}}\right]\times\check{p}(x_0,\boldsymbol{\kappa})\,d^2\kappa. \tag{88}$$

This formula expresses the split-step spectral algorithm for the EWAPE in a 3D moving medium for case (i) considered in the Introduction. If $v = 0$, Eq. (88) coincides with Eq. (34) obtained for a motionless medium.

To check the results, consider a plane wave incident on the 3D slab with constant ε, $\tilde{\varrho}$, and $\mathbf{v}$ (Fig. 1). Substituting Eq. (55) into Eq. (88), we obtain the sound field of this wave at the right boundary of the slab, $p = A\exp(\Phi_m)$, where Φ_m is the phase increment in a moving medium,

$$\Phi_m(x,\mathbf{r}) = \boldsymbol{\kappa}_0\cdot\mathbf{r} + i\Delta x\sqrt{k_0^2-\kappa_0^2} + i\Delta x k_0^2\frac{\varepsilon(x_0,\mathbf{r}) - 2\mathbf{s}(\boldsymbol{\kappa}_0)\cdot\mathbf{v}/c_0}{2\sqrt{k_0^2-\kappa_0^2}}. \tag{89}$$

Here, the sum of the first two terms is equal to $k_0 L$ and in the third term, $k_0\Delta x/(k_0^2-\kappa_0^2)^{1/2} = \Delta x/\cos\theta_0 = L$. Thus, the phase increment can be written as

$$\Phi_m = k_0 L + k_0 L[\varepsilon/2 - \mathbf{s}(\boldsymbol{\kappa}_0)\cdot\mathbf{v}/c_0]. \tag{90}$$

The phase increment of this plane wave can also be calculated using geometrical acoustics. In this case, the phase increment can be determined with Eq. (3.57) in Ref. 11, namely

$$\Phi_m = \frac{k_0 c_0 L}{|c\mathbf{n} + \mathbf{v}|}. \tag{91}$$

Here, $\mathbf{n}$ is the unit vector perpendicular to the wave front of the plane wave in the 3D slab. To order v/c, Eq. (91) can be written as

$$\Phi_m = k_0 L\left(\frac{c_0}{c} - \frac{\mathbf{n}\cdot\mathbf{v}}{c}\right). \tag{92}$$

In this formula, $c_0/c = 1 + \varepsilon/2 + O(\varepsilon^2)$. In the last term in Eq. (92), we take into account that $c = c_0(1 - \varepsilon/2 + O(\varepsilon^2))$ and $\mathbf{n} = \mathbf{s} + O(\varepsilon, v/c_0)$. Since the derivations are done to order $O(\varepsilon, v/c_0)$, Eq. (92) becomes

$$\Phi_m = k_0 L + k_0 L(\varepsilon/2 - \mathbf{s}\cdot\mathbf{v}/c_0), \tag{93}$$

which coincides with Eq. (90). Thus, for the problem considered here, the phase increment in the split-step spectral algorithm coincides with that in the geometrical acoustics approximation.

D. EWAPE in a moving medium

Equation (88) is the split-step spectral algorithm in a moving medium. Starting with this equation, similarly to Sec. IV, we can derive the EWAPE corresponding to this algorithm.

In Eq. (88), the dot product can be written as

$$\mathbf{s}(\boldsymbol{\kappa})\cdot\mathbf{v} = v_x\sqrt{1 - \kappa^2/k_0^2} + \mathbf{v}_\perp\cdot\boldsymbol{\kappa}/k_0. \tag{94}$$

Using this formula and applying the operator $\partial/\partial x$ to both sides of Eq. (88), we obtain

$$\begin{aligned}\frac{\partial p(x,\mathbf{r})}{\partial x} = i\int\Bigg[&\sqrt{k_0^2 - \kappa^2} - k_0\frac{v_x}{c_0} + k_0^2\left(\frac{\varepsilon}{2} - \frac{\mathbf{v}_\perp}{c_0}\cdot\frac{\boldsymbol{\kappa}}{k_0}\right)\\ &\times\left(k_0^2 - \kappa^2\right)^{-1/2}\Bigg]\\ &\times\exp\Bigg[i\boldsymbol{\kappa}\cdot\mathbf{r} + i\Delta x\sqrt{k_0^2 - \kappa^2} + i\Delta x k_0^2\\ &\times\frac{\varepsilon(x_0,\mathbf{r}) - 2\mathbf{s}(\boldsymbol{\kappa})\cdot\mathbf{v}(x_0,\mathbf{r})/c_0}{2\sqrt{k_0^2 - \kappa^2}}\Bigg]\check{p}(x_0,\boldsymbol{\kappa})\,d^2\kappa.\end{aligned} \tag{95}$$

The first term in the integrand can be factored out from the integral similarly to that in Eq. (37). The remaining integral is equal to p. As a result, we obtain

$$\begin{aligned}&\left(\frac{\partial}{\partial x} - ik_0\sqrt{1+\hat{\mu}}\right)p + ik_0\frac{v_x}{c_0}p\\ &\quad - ik_0\left(\frac{\varepsilon}{2} + \frac{i}{k_0}\frac{\mathbf{v}_\perp}{c_0}\cdot\frac{\partial}{\partial\mathbf{r}}\right)(1+\hat{\mu})^{-1/2}p = 0.\end{aligned} \tag{96}$$

This is a new result. Equation (96) is the EWAPE in a 3D moving medium valid for case (i) considered in the Introduction. It would be difficult to derive this equation starting from Eq. (21) and using the substitution, Eq. (69). Equation (88) can be now recognized as a split-step spectral algorithm for solving Eq. (96).

In the limiting cases, the EWAPE given by Eq. (96) coincides with equations known in the literature. If $\mathbf{v} = 0$, Eq. (96) becomes EWAPE1 for a motionless medium, Eq. (21), where the derivatives of ε are omitted. In the narrow-angle approximation, the first square root in Eq. (96) can be approximated as $1 + \hat{\mu}/2$, while $(1+\hat{\mu})^{-1/2} \approx 1$. The result is

$$\begin{aligned}&\frac{\partial p}{\partial x} - ik_0(1 + \hat{\mu}/2)p + ik_0\frac{v_x}{c_0}p\\ &\quad - ik_0\left(\frac{\varepsilon}{2} + \frac{i}{k_0}\frac{\mathbf{v}_\perp}{c_0}\cdot\frac{\partial}{\partial\mathbf{r}}\right)p = 0.\end{aligned} \tag{97}$$

Substituting with $p = \exp(ik_0 x)A$, this equation reduces to the narrow-angle PE for the complex amplitude A of the sound pressure in a moving medium, which coincides with Eq. (2.110) in Ref. 11. This derivation clearly shows the importance of the term involving the transverse medium velocity $\mathbf{v}_\perp$ in Eq. (96), which is sometimes omitted in the literature.

Approximating the square roots in Eq. (96) with Padé (n,n) series, we obtain a WAPE for sound propagation in a moving medium,

$$\begin{aligned}&\left[\frac{\partial}{\partial x} - ik_0\left(1 + \sum_{j=1}^{n}\frac{a_{j,n}\hat{\mu}}{1 + b_{j,n}\hat{\mu}}\right)\right]p + ik_0\frac{v_x}{c_0}p\\ &\quad - ik_0\left(\frac{\varepsilon}{2} + \frac{i}{k_0}\frac{\mathbf{v}_\perp}{c_0}\cdot\frac{\partial}{\partial\mathbf{r}}\right)\quad 1 + \sum_{j=1}^{n}\frac{\tilde{a}_{j,n}\hat{\mu}}{1 + \tilde{b}_{j,n}\hat{\mu}}\Bigg)p = 0.\end{aligned} \tag{98}$$

Here, the coefficients a_j, b_j, $\tilde{a}_j$, and $\tilde{b}_j$ coincide with those in Eq. (53) for a motionless medium. Equation (98) is also a new result obtained here. It can be solved numerically by algorithms developed for a motionless medium.[4] For the Padé (1,1) approximation, due to the high-frequency approximation, Eq. (98) is much simpler than the WAPEs in Refs. 7 and 8.

VIII. CONCLUSIONS

This paper provided a new approach for WAPEs, which are widely used in physics. The starting point of the analysis was the EWAPE (17), termed EWAPE1, which is valid for small variations in the refractive index of a medium. As these variations decrease, EWAPE1 accounts correctly for propagation angles up to 90° with respect to the nominal direction. The operator form, Eq. (21), of EWAPE1 was derived. This equation was then generalized for large variations in the refractive index, resulting in EWAPE2, Eq. (24).

For a relatively small range, EWAPE1 was solved by a perturbation technique. The resulting formula, Eq. (30), expresses the sound pressure at the right boundary of a 3D slab in terms of the Fourier transform of the sound pressure at its left boundary and the wide-angle phase factor due to the refractive index variations. This approach is termed as a split-step spectral algorithm for EWAPE1. The approach simplifies in the high-frequency approximation, when the

wide-angle phase factor is evaluated analytically, Eq. (34). Numerical implementation of the split-step spectral algorithm was discussed. Generally, the approach is more computationally intensive than a PE and GFPE but perhaps can be improved in the future. Currently it can be used if very wide propagation angles need to be accounted for when other WAPEs do not provide sufficient accuracy. The split-step spectral algorithm was also applied for EWAPE2.

It was shown that under certain approximations, the two EWAPEs and the corresponding split-step spectral algorithms reduce to WAPEs known in the literature. This is an important methodological result, as it provides an alternative derivation of the WAPEs and enables better understanding of the underlying physics and ranges of applicability of these equations. In particular, it was shown the WAPEs known in the literature can be obtained by approximating the wave vectors and propagation paths of the plane waves in the spectral decomposition of the sound pressure at the right boundary of the 3D slab. This provides a clear physical meaning of approximations pertinent to the WAPEs and enables analysis of their ranges of applicability. The ranges of applicability of the EWAPEs and WAPEs were studied for a plane wave propagating through a homogeneous 3D slab. It was shown that the EWAPEs are applicable for larger propagation angles than WAPEs and GFPE used in the literature.

Based on the EWAPEs and split-step spectral algorithm, new WAPEs can be derived. As an example, Eq. (53) was obtained and might be simpler than the WAPE used in the literature, Eqs. (5) and (8). Also, it was emphasized that the GFPE, Eq. (67), which is used in atmospheric acoustics for sound propagation above an impedance ground, employs a narrow-angle phase factor due to the refractive index variations. The extra-wide-angle GFPEs, Eqs. (64) and (66), were suggested.

Sound propagation in both motionless and moving media was considered. In the latter case, the split-step spectral algorithm for EWAPE1 significantly simplifies the formulation by replacing many partial derivatives of the sound pressure, medium velocity, and density appearing in a WAPE with the wave vectors (essentially, propagation angles) in the spectral domain. In the high-frequency approximation, a new EWAPE in a moving medium, Eq. (96), and the split-step spectral algorithm for its solution, Eq. (88), were derived. For narrow-angle propagation, Eq. (96) reduces to the conventional PE, Eq. (97). The derivation emphasizes that in a moving medium, the PE should contain a term proportional to the wind velocity component perpendicular to the propagation path, which is sometimes omitted in the literature. Based on the formalism developed, a new WAPE for sound propagation in a moving medium, Eq. (98), was derived. In subsequent research, we intend to solve numerically this equation by approaches developed for a motionless medium (e.g., Ref. 4).

Most formulations presented here were for 3D sound propagation. Section V outlined how the results can be applied to the 2D case.

ACKNOWLEDGMENTS

This research was sponsored by the U.S. Army Engineer Research and Development Center, Geospatial Research and Engineering and Military Engineering business areas.

APPENDIX A: POINT SOURCE IN A STRATIFIED MEDIUM

In this appendix, we consider the sound field of a point source in a stratified medium in which $\varepsilon = \varepsilon(x)$. As indicated in Sec. III C, this problem is pertinent to an acoustic source located above the ground and a ground-based receiver, or vice versa. For this problem, the sound pressure is calculated with the two EWAPEs and then compared with that obtained with the Helmholtz equation.

Without loss of generality, we assume that the point source is located at the origin of the coordinate system shown in Fig. 1 and that $x_0 = 0$ in the figure. Starting with EWAPE2, the sound pressure at the plane $x = \text{const}$ can be calculated similarly to that in Sec. IV C. The result coincides with Eq. (42) in which $x_0 = 0$,

$$p(x,\mathbf{r}) = \int \exp\left[i\boldsymbol{\kappa}\cdot\mathbf{r} + i\int_0^x \sqrt{k_0^2(1+\varepsilon(x')) - \kappa^2}\,dx'\right] \times \check{p}(0,\boldsymbol{\kappa})\,d^2\kappa. \tag{A1}$$

Here, $\check{p}(0,\boldsymbol{\kappa})$ is the Fourier transform of the sound pressure due to the point source in the plane $x = 0$. This Fourier transform can be found by comparing Eqs. (11) and (13), $\check{p}(0,\boldsymbol{\kappa}) = i/(2\pi\sqrt{k_0^2-\kappa^2})$. Substituting this result into Eq. (A1), we have

$$p(x,\mathbf{r}) = \frac{i}{2\pi}\int \exp\left[i\boldsymbol{\kappa}\cdot\mathbf{r} + i\int_0^x \sqrt{k_0^2(1+\varepsilon(x')) - \kappa^2}\,dx'\right] \times \frac{d^2\kappa}{\sqrt{k_0^2-\kappa^2}}. \tag{A2}$$

In this equation, the integral can be evaluated with the 2D method of a stationary phase (e.g., Sec. 4.4.4 in Ref. 11). The 2D stationary point $\boldsymbol{\kappa}_0$ is determined from the equation $\partial\Phi/\partial\boldsymbol{\kappa}_0 = 0$, where Φ is the phase in the exponential in Eq. (A2). This equation can be written in the form

$$\mathbf{r} = \boldsymbol{\kappa}_0\int_0^x \frac{dx'}{\sqrt{k_0^2(1+\varepsilon(x')) - \kappa_0^2}}. \tag{A3}$$

For the given receiver coordinates $(x, \mathbf{r})$, this equation defines the stationary point $\boldsymbol{\kappa}_0$. Note that Eq. (A3) also determines the sound ray path $\mathbf{r} = \mathbf{r}(x)$ in a stratified medium. Applying the 2D method of stationary phase to Eq. (A2), we obtain

$$p(x,\mathbf{r}) = \frac{1}{\sqrt{k_0^2-\kappa_0^2}\,J^{1/2}} \times \exp\left[i\boldsymbol{\kappa}_0\cdot\mathbf{r} + i\int_0^x \sqrt{k_0^2(1+\varepsilon(x')) - \kappa_0^2}\,dx'\right], \tag{A4}$$

where the function J is given by

$$J = k_0^2 \int_0^x \frac{dx'}{\sqrt{k_0^2(1+\varepsilon(x')) - \kappa_0^2}} \int_0^x \frac{[1+\varepsilon(x')]dx'}{\left[k_0^2(1+\varepsilon(x')) - \kappa_0^2\right]^{3/2}}. \tag{A5}$$

Equation (A4) expresses the sound pressure due to the point source in a stratified medium obtained with EWAPE2.

For the same problem, the sound pressure is also calculated in Ref. 11 starting with the Helmholtz equation (1) and using the high-frequency approximation. In the absence of turning points, the sound pressure is given by Eq. (4.53) in that reference,

$$p(x,\mathbf{r}) = \frac{1}{\left[k_0^2(1+\varepsilon(x)) - \kappa_0^2\right]^{1/4} \left[k_0^2(1+\varepsilon(0)) - \kappa_0^2\right]^{1/4} J^{1/2}} \times \exp\left[i\boldsymbol{\kappa}_0 \cdot \mathbf{r} + i\int_0^x \sqrt{k_0^2(1+\varepsilon(x')) - \kappa_0^2}\, dx'\right]. \tag{A6}$$

Here, $\boldsymbol{\kappa}_0$ and J are defined with Eqs. (A3) and (A5), and without loss of generality, $\varepsilon(0)$ can be set to zero by redefining the reference wavenumber k_0. Comparing Eqs. (A4) and (A6), we conclude that the phases of the sound pressures are the same, while the amplitudes are different. The ratio of the amplitudes in these equations is given by

$$R_p(x,\mathbf{r}) = \left(1 + \frac{\varepsilon(x)}{1 - \kappa_0^2/k_0^2}\right)^{1/4}. \tag{A7}$$

According to this formula, the ratio of the amplitudes increases with increasing ε and increasing the propagation angle θ when κ_0 tends to k_0. The difference in the amplitudes might be due to the omission of the commutator $[\partial/\partial x, \hat{Q}]$ in EWAPE2.

Similarly, the sound pressure due to the point source can be calculated with EWAPE1. The result is

$$p(x,\mathbf{r}) = \frac{1}{\sqrt{k_0^2 - \tilde{\kappa}_0^2}\,\tilde{J}^{1/2}} \exp\left[i\tilde{\boldsymbol{\kappa}}_0 \cdot \mathbf{r} + ix\sqrt{k_0^2 - \tilde{\kappa}_0^2} + i\frac{k_0^2}{2\sqrt{k_0^2 - \tilde{\kappa}_0^2}} \int_0^x \varepsilon(x')\, dx'\right]. \tag{A8}$$

Here, the 2D stationary point $\tilde{\boldsymbol{\kappa}}_0$ is determined with the equation

$$\mathbf{r} = \frac{\tilde{\boldsymbol{\kappa}}_0}{\sqrt{k_0^2 - \tilde{\kappa}_0^2}} \left[x - \frac{k_0^2}{2(k_0^2 - \tilde{\kappa}_0^2)} \int_0^x \varepsilon(x')\, dx'\right], \tag{A9}$$

and the function $\tilde{J}$ is given by

$$\tilde{J} = \frac{k_0^2 x}{(k_0^2 - \tilde{\kappa}_0^2)^2} \left[x - \frac{k_0^2 + \tilde{\kappa}_0^2}{k_0^2 - \tilde{\kappa}_0^2} \int_0^x \varepsilon(x')\, dx'\right]. \tag{A10}$$

Equations (A8)–(A10) can also be obtained from the corresponding results for EWAPE2 by keeping the first two terms in the square-root expansion with respect to the small parameter ε. This correspondence between EWAPE1 and EWAPE2 is also valid for other results obtained in the paper.

APPENDIX B: DERIVATION OF EQ. (78)

In this appendix, Eq. (78) is derived.

Consider one of the integrals with respect to $\mathbf{r}_1$ appearing in Eq. (76),

$$I_r = \int \frac{\partial \tilde{\varrho}(x_1, \mathbf{r}_1)}{\partial \mathbf{r}_1} \exp[i(\boldsymbol{\kappa} - \boldsymbol{\kappa}_1) \cdot \mathbf{r}_1]\, d^2 r_1. \tag{B1}$$

This integral can be written as

$$I_r = \int \left\{ \frac{\partial}{\partial \mathbf{r}_1} \left[\tilde{\varrho}(x_1, \mathbf{r}_1) \exp[i(\boldsymbol{\kappa} - \boldsymbol{\kappa}_1) \cdot \mathbf{r}_1]\right] - i(\boldsymbol{\kappa} - \boldsymbol{\kappa}_1)\tilde{\varrho}(x_1, \mathbf{r}_1) \exp[i(\boldsymbol{\kappa} - \boldsymbol{\kappa}_1) \cdot \mathbf{r}_1] \right\} d^2 r_1. \tag{B2}$$

Assuming that $\tilde{\varrho}$ vanishes at infinity, the first integral can be neglected. The same result follows from the divergence theorem. Comparing the right-hand sides of Eqs. (B1) and (B2), we obtain

$$\frac{\partial \tilde{\varrho}(x_1, \mathbf{r}_1)}{\partial \mathbf{r}_1} \to i(\boldsymbol{\kappa}_1 - \boldsymbol{\kappa})\tilde{\varrho}(x_1, \mathbf{r}_1). \tag{B3}$$

Consider now one of the integrals with respect to x_1 appearing in Eq. (76),

$$I_x = \int_{x_0}^x \frac{\partial \tilde{\varrho}(x_1, \mathbf{r}_1)}{\partial x_1} e^{i(x - x_1)\eta}\, dx_1, \tag{B4}$$

where $\eta = \sqrt{k_0^2 - \kappa_1^2} - \sqrt{k_0^2 - \kappa^2}$. This integral can be written as

$$I_x = \int_{x_0}^x \left\{ \frac{\partial}{\partial x_1} \left[\tilde{\varrho}(x_1, \mathbf{r}_1) e^{i(x - x_1)\eta}\right] + i\eta \tilde{\varrho}(x_1, \mathbf{r}_1) e^{i(x - x_1)\eta} \right\} dx_1. \tag{B5}$$

The first of the integrals on the right-hand side can be evaluated as

$$I_{x,1} = \tilde{\varrho}(x, \mathbf{r}_1) - \tilde{\varrho}(x_0, \mathbf{r}_1) e^{i\Delta x \eta} \approx \tilde{\varrho}(x, \mathbf{r}_1) - \tilde{\varrho}(x_0, \mathbf{r}_1) \approx \Delta x \frac{\partial \tilde{\varrho}(x_0, \mathbf{r}_1)}{\partial x_0} \sim \Delta x \tilde{\varrho}(x_0, \mathbf{r}_1)/l, \tag{B6}$$

where l is a characteristic scale of the density variations. The second integral in Eq. (B5) can be estimated as

$$I_{x,2} \sim \Delta x \eta \tilde{\varrho}(x_0, \mathbf{r}_1) \sim \Delta x k_0 \sin\theta\, \tilde{\varrho}(x_0, \mathbf{r}_1). \tag{B7}$$

Here, θ is a characteristic angle of sound propagation with respect to the x axis. In the high-frequency approximation, $I_{x,1}$ can be ignored in comparison with $I_{x,2}$. Comparing the right-hand sides of Eqs. (B4) and (B5), we obtain

$$\frac{\partial \tilde{\varrho}(x_1, \mathbf{r}_1)}{\partial x_1} \to i\left(\sqrt{k_0^2 - \kappa_1^2} - \sqrt{k_0^2 - \kappa^2}\right)\tilde{\varrho}(x_1, \mathbf{r}_1). \tag{B8}$$

Combining Eqs. (B3) and (B8), we obtain Eq. (78). The same result can be obtained for the velocity terms.

[1]J. F. Claerbout, *Fundamentals of Geophysical Data Processing* (Blackwell, Oxford, 1985), pp. 194–207.

[2]F. D. Tappert, "The parabolic approximation method," in *Wave Propagation in Underwater Acoustics*, edited by J. B. Keller and J. S. Papadakis (Springer, New York, 1977), pp. 224–287.

[3]D. Lee and S. T. McDaniel, *Ocean Acoustic Propagation by Finite Difference Methods* (Pergamon, New York, 1988), pp. 305–423.

[4]M. D. Collins, "A split-step Padé solution for the parabolic equation method," J. Acoust. Soc. Am. **93**, 1736–1742 (1993).

[5]F. B. Jensen, W. A. Kuperman, M. B. Porter, and H. Schmidt, *Computational Ocean Acoustics*, second ed. (Springer, New York, 2011), pp. 457–529.

[6]O. A. Godin, "Wide-angle parabolic equations for sound in a 3D inhomogeneous moving medium," Doklady Phys. **47**(9), 643–646 (2002).

[7]V. E. Ostashev, D. Juvé, and P. Blanc-Benon, "Derivation of a wide-angle parabolic equation for sound waves in inhomogeneous moving media," Acta Acust. Acust. **83**(3), 455–460 (1997).

[8]Ph. Blanc-Benon, L. Dallois, and D. Juvé, "Long range sound propagation in a turbulent atmosphere within the parabolic approximation," Acta Acust. Acust. **87**(6), 659–669 (2001).

[9]E. Salomons, *Computational Atmospheric Acoustics* (Kluwer Academic, Dordrecht, 2001), pp. 181–202.

[10]J. F. Lingevitch, M. D. Collins, D. K. Dacol, D. P. Drob, J. C. W. Rogers, and W. L. Siegmann, "A wide angle and high Mach number parabolic equation," J. Acoust. Soc. Am. **111**, 729–734 (2002).

[11]V. E. Ostashev and D. K. Wilson, *Acoustics in Moving Inhomogeneous Media*, second ed. (CRC Press, Boca Raton, FL, 2015), 521 pp.

[12]F. Dagrau, M. Rénier, R. Marchiano, and F. Coulouvrat, "Acoustic shock wave propagation in a heterogeneous medium: A numerical simulation beyond the parabolic approximation," J. Acoust. Soc. Am. **130**, 20–32 (2011).

[13]L.-J. Gallin, M. Rénier, É. Gaudard, Th. Farges, R. Marchiano, and F. Coulouvrat, "One-way approximation for the simulation of weak shock wave propagation in atmospheric flows," J. Acoust. Soc. Am. **135**, 2559–2570 (2014).

[14]S. M. Rytov, Yu. A. Kravtsov, and V. I. Tatarskii, *Principles of Statistical Radio Physics. Part 4, Wave Propagation through Random Media* (Springer, Berlin, 1989), 188 pp.

[15]C. L. Rino, *The Theory of Scintillation with Applications in Remote Sensing* (IEEE, Piscataway, NJ, 2011), 226 pp.

[16]M. D. Feit and J. A. Fleck, "Light propagation in graded-index optical fibers," Appl. Opt. **17**, 3990–3998 (1978).

[17]V. E. Ostashev and V. I. Tatarskii, "A series based on back-scattering multiplicity in problems of wave propagation in inhomogeneous media," in *Proceedings of the 8th Symposium on Diffraction and Wave Propagation*, Moscow (1977), Part 1, pp. 315–318.

[18]V. E. Ostashev and V. I. Tatarskii, "A series based on multiple backscattering in problems of wave propagation in inhomogeneous media," Radiophys. Quantum. Electron. **21**(5), 504–513 (1978).

[19]R. Cheng, P. J. Morris, and K. S. Brentner, "A three dimensional parabolic equation method for sound propagation in moving inhomogeneous media," J. Acoust. Soc. Am. **126**, 1700–1710 (2009).

[20]F. Sturm, "Leading-order cross term correction of three-dimensional parabolic equation models," J. Acoust. Soc. Am. **139**, 263–270 (2016).

[21]D. J. Thomson and N. R. Chapman, "A wide-angle split-step algorithm for the parabolic equation," J. Acoust. Soc. Am. **74**(6), 1848–1854 (1983).

[22]L. Halpern and L. N. Trefethen, "Wide-angle one-way wave equations," J. Acoust. Soc. Am. **84**, 1397–1404 (1988).

[23]V. E. Ostashev and V. I. Tatarskii, "Representation of the Helmholtz equation solution in the form of a series based on backscattering multiplicity," Waves Random Media **5**, 125–135 (1995).

[24]M. B. Muhlestein, V. E. Ostashev, and D. K. Wilson, "A Green's function parabolic equation description of infrasound propagation in an inhomogeneous and moving atmosphere," J. Acoust. Soc. Am. **143**(3), 1740 (2018).

[25]K. E. Gilbert and X. Di, "A fast Green's function method for one-way sound propagation in the atmosphere," J. Acoust. Soc. Am. **94**, 2343–2352 (1993).

[26]K. E. Gilbert, "Eigenfunction approach to the Green's function parabolic equation in outdoor sound: A tutorial," J. Acoust. Soc. Am. **139**(3), 1071–1080 (2016).

[27]V. E. Ostashev, Ph. Blanc-Benon, D. Júve, and L. Dallois, "Wide angle parabolic equation for sound waves in a refractive, turbulent atmosphere," in *Proceedings of the 10th International Symposium on Long Range Sound Propagation*, Grenoble, France, 2002, pp. 62–72.

REPORT DOCUMENTATION PAGE

Form Approved
OMB No. 0704-0188

1. REPORT DATE *(DD-MM-YYYY)*	2. REPORT TYPE	3. DATES COVERED *(From - To)*
September 2021	Final	

4. TITLE AND SUBTITLE

Extra-Wide-Angle Parabolic Equations in Motionless and Moving Media

5a. CONTRACT NUMBER

5b. GRANT NUMBER

5c. PROGRAM ELEMENT NUMBER

6. AUTHOR(S)

Vladimir E. Ostashev, Michael B. Muhlestein, and D. Keith Wilson

5d. PROJECT NUMBER

5e. TASK NUMBER

5f. WORK UNIT NUMBER

7. PERFORMING ORGANIZATION NAME(S) AND ADDRESS(ES)

Cold Regions Research and Engineering Laboratory
U.S. Army Engineer Research and Development Center
72 Lyme Road
Hanover, NH 03755

8. PERFORMING ORGANIZATION REPORT NUMBER

ERDC/CRREL MP-21-22

9. SPONSORING / MONITORING AGENCY NAME(S) AND ADDRESS(ES)

U.S. Army Corps of Engineers
Washington, DC 20314

10. SPONSOR/MONITOR'S ACRONYM(S)

USACE

11. SPONSOR/MONITOR'S REPORT NUMBER(S)

12. DISTRIBUTION / AVAILABILITY STATEMENT

Approved for public release; distribution is unlimited.

13. SUPPLEMENTARY NOTES

This article was originally published online in the *Journal of the Acoustical Society of America* on 25 February 2019.
This research was sponsored by the U.S. Army Engineer Research and Development Center, Geospatial Research and Engineering and Military Engineering business areas.

14. ABSTRACT

Wide-angle parabolic equations (WAPEs) play an important role in physics. They are derived by an expansion of a square-root pseudo-differential operator in one-way wave equations, and then solved by finite-difference techniques. In the present paper, a different approach is suggested. The starting point is an extra-wide-angle parabolic equation (EWAPE) valid for small variations of the refractive index of a medium. This equation is written in an integral form, solved by a perturbation technique, and transformed to the spectral domain. The resulting split-step spectral algorithm for the EWAPE accounts for the propagation angles up to 90° with respect to the nominal direction. This EWAPE is also generalized to large variations in the refractive index. It is shown that WAPEs known in the literature are particular cases of the two EWAPEs. This provides an alternative derivation of the WAPEs, enables a better understanding of the underlying physics and ranges of their applicability, and opens an opportunity for innovative algorithms. Sound propagation in both motionless and moving media is considered. The split-step spectral algorithm is particularly useful in the latter case since complicated partial derivatives of the sound pressure and medium velocity reduce to wave vectors (essentially, propagation angles) in the spectral domain.

15. SUBJECT TERMS

Sound-waves; Sound—Propagation; Physics; Differential equations; Parabolic

16. SECURITY CLASSIFICATION OF:			17. LIMITATION OF ABSTRACT	18. NUMBER OF PAGES	19a. NAME OF RESPONSIBLE PERSON
a. REPORT	b. ABSTRACT	c. THIS PAGE			19b. TELEPHONE NUMBER *(include area code)*
Unclassified	Unclassified	Unclassified	UU	22	